



The SIS100 Dipole Magnet

Egbert Fischer, Pierre Schnizer

MAC-3

February 10 - 12, 2010

GSI, Darmstadt

The SIS100 Dipole Magnet: Contents

1. Introduction
2. Main magnet components
3. Mechanical stability of the coil windings
4. Magnetic steel
5. Magnetic field design
6. Losses and hydraulic limits
7. Vacuum chamber and temperature fields
8. Milestones towards a curved single layer dipole
9. Conclusion

The references to the original papers are omitted in this presentation as there content is summarised as well as referenced in the distributed report:

E. Fischer, P. Schnizer:

Design and Test Status of the SIS100 Dipole Magnet



1. Introduction

2. Main magnet components
3. Mechanical stability of the coil windings
4. Magnetic steel
5. Magnetic field design
6. Losses and hydraulic limits
7. Vacuum chamber and temperature fields
8. Milestones towards a curved single layer dipole
9. Conclusion

Introduction: Design principles

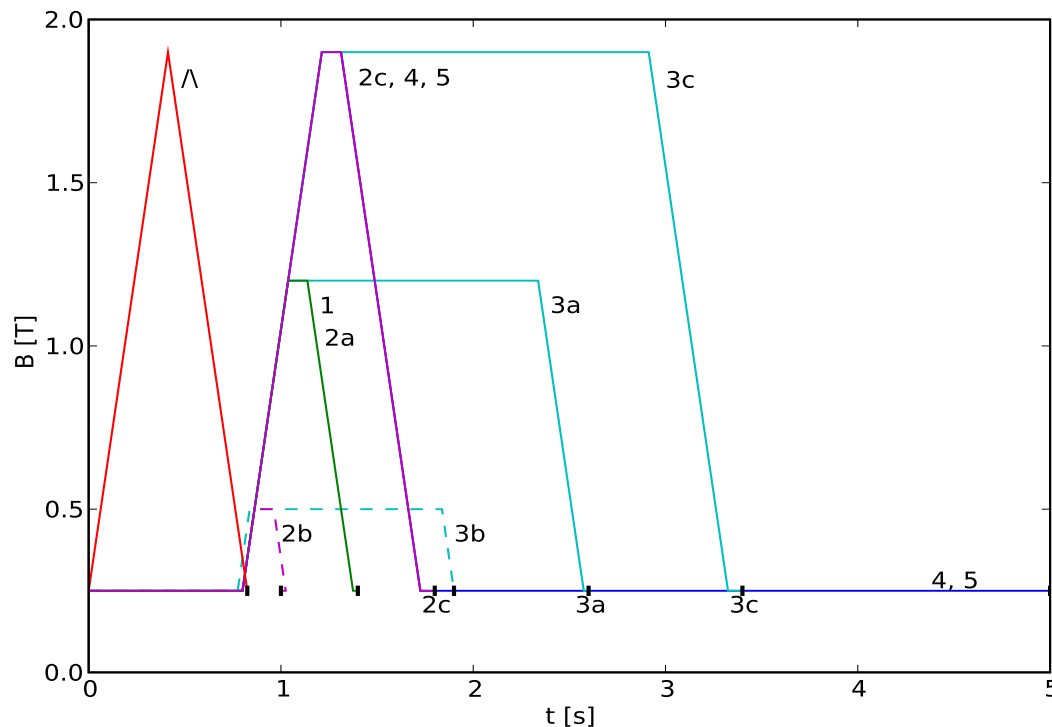
- simple magnet design
- coil cooled by two phase Helium flow
- straightforward robust magnet yoke
- start from Nuclotron design

	unit	Nuclotron	S2LD BNG	C2LD BINP	Curved dipole
$B \times L_{\text{effective}}$	[Tm]	2.823	5.788	5.819	5.818
B_{max}	[T]	1.98	2.1	1.9	1.9
$L_{\text{effective}}$	[m]	1.426	2.756	3.062	3.062
Estimated L_{yoke}	[m]	1.370	2.731	3.002	3.002
Bending angle	[deg]	3.75	3.33	3.33	3.33
Radius of curvature	[m]	22.5	47.368	52.632	52.632
Usable aperture (h x v)	[mm]	110 x 55	130 x 60	113 x 58	120 x 60

Introduction: Requirements

- a field strength curvature of $B_p = 100$ [Tm]
- good field region: an ellipse $a = 57.5$ mm, $b = 30$ mm

Main operation cycles



Cycle	B_{\max} [T]	t_f [s]	t_c [s]
1	1.2	0.1	1.4
2a	1.2	0.1	1.4
2b	0.5	0.1	1
2c	1.9	0.1	1.8
3a	1.2	1.3	2.6
3b	0.5	1.0	1.9
3c	1.9	1.7	3.4
4	1.9	0.1	5.0
5	1.9	0.1	5.0
Λ	1.9	0	0.84



1. Introduction

2. Main magnet components

- Curved single layer dipole
- First full size magnet

3. Mechanical stability of the coil windings

4. Magnetic steel

5. Magnetic field design

6. Losses and hydraulic limits

7. Vacuum chamber and temperature fields

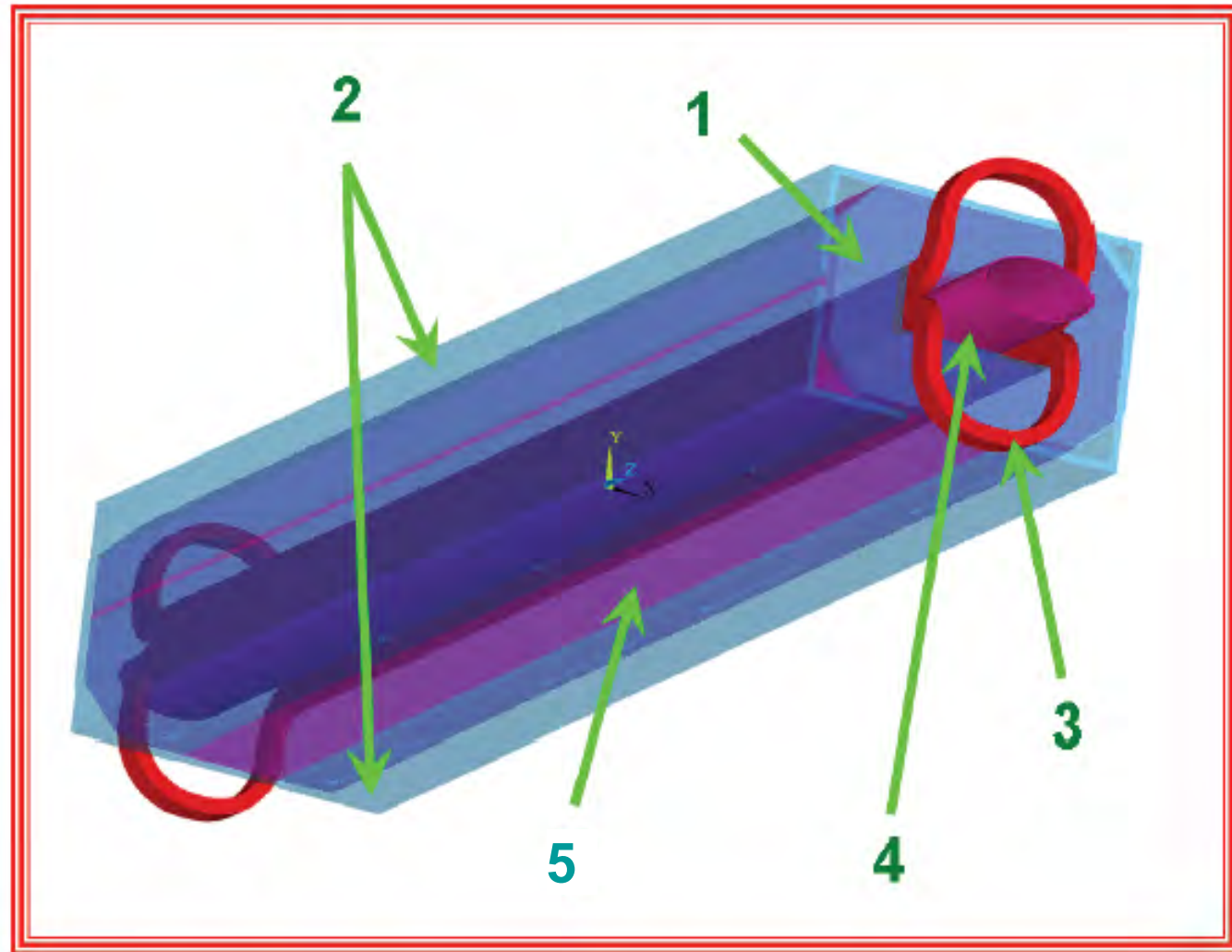
8. Milestones towards a curved single layer dipole

9. Conclusion

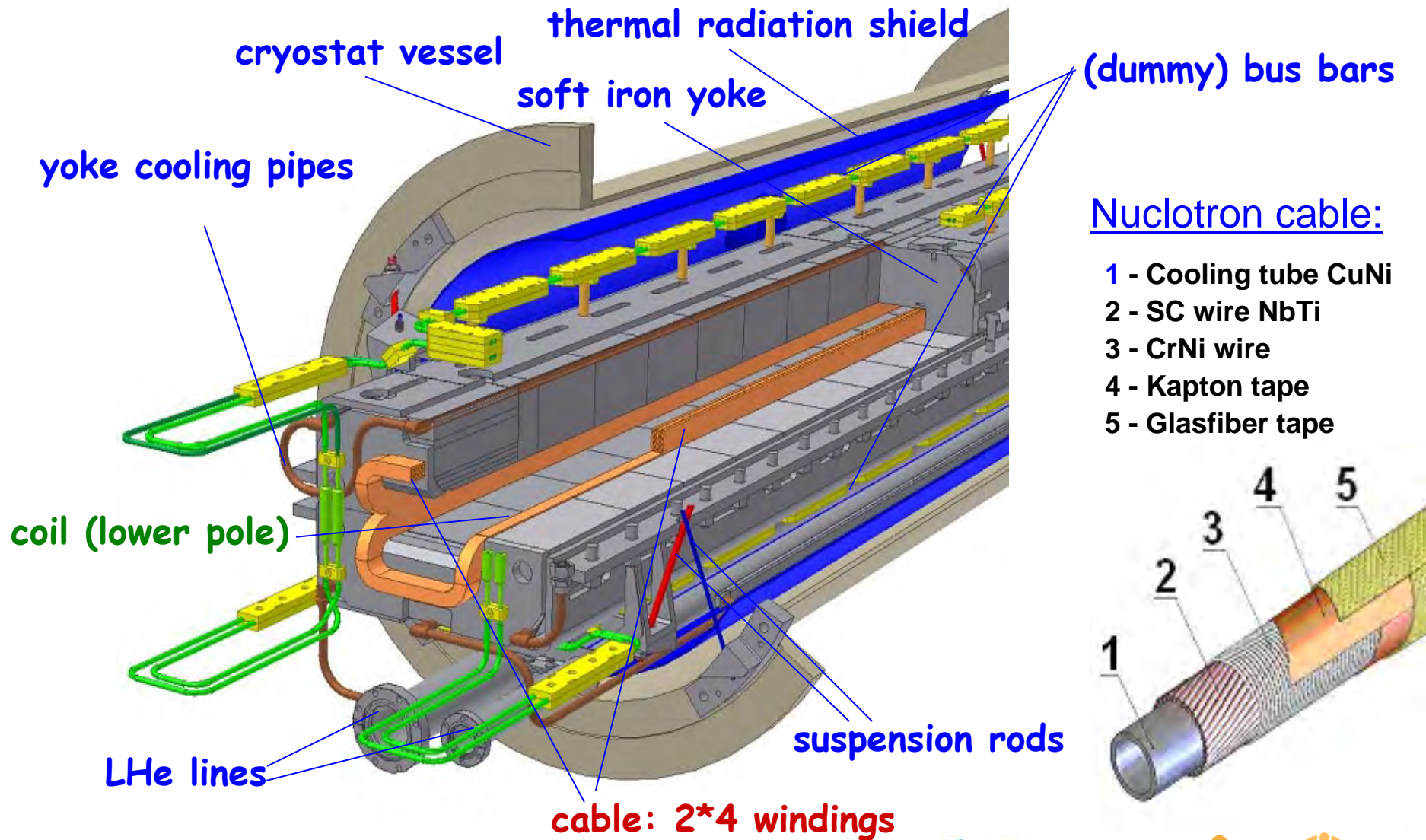
Main magnet components

ANSYS Model:

- 1 – yoke end plate
- 2 – brackets
- 3 – coil end loop
- 4 – beam pipe
- 5 – laminated yoke



Main magnet components: Layout 1st dipole

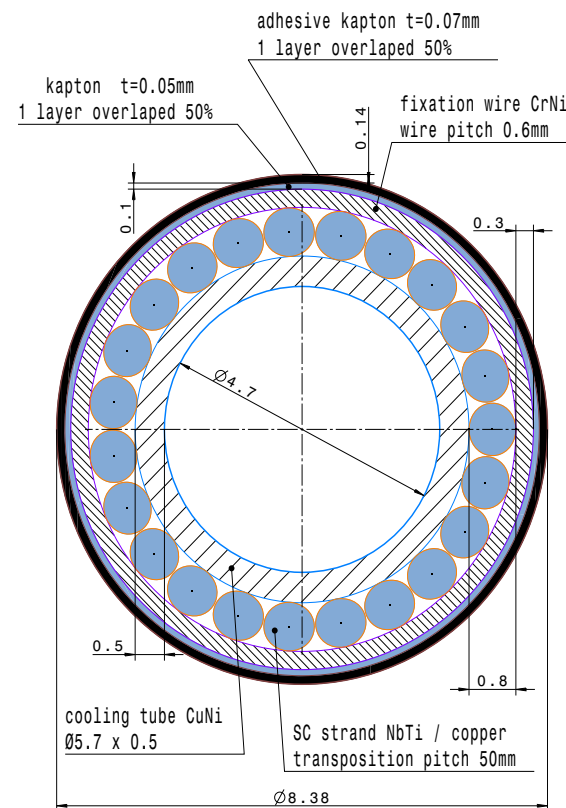


Main magnet components: Dipole parameters

Number of magnets		108 + 1 reference magnet
Design		Window-frame, laminated cold iron yoke, lamination thickness 1mm, one layer coil with 8 turns
Max. Field	T	1.9
Min. Field	T	0.23
Bending angle	Deg.	3.33
Edge angles (entrance / exit)	Deg.	1.665 / -1.665
Orbit curvature radius, R	m	52.632
Effective magnetic length, L	m	3.062
Coil aperture	mm	165 · 68
Useable aperture (good field region):	mm mm	120 · 60 115 · 60
Field quality (goal)		$\pm 6 \cdot 10^{-4}$
Current at max. field	A	12745
Inductance	mH	0.55
Ramp rate	T/s	4
Cycle 2c		
Cycle length	s	1.735
High field flat top duration	s	0.1
Low field flat top duration	s	0.8
AC loss @4.2K per magnet (cycle number 2c)	W	35.7
Overall width (cryostat)	m	1.0
Overall height (cryostat)	m	1.0
Overall weight	kg	1850

Main magnet components: High current cable

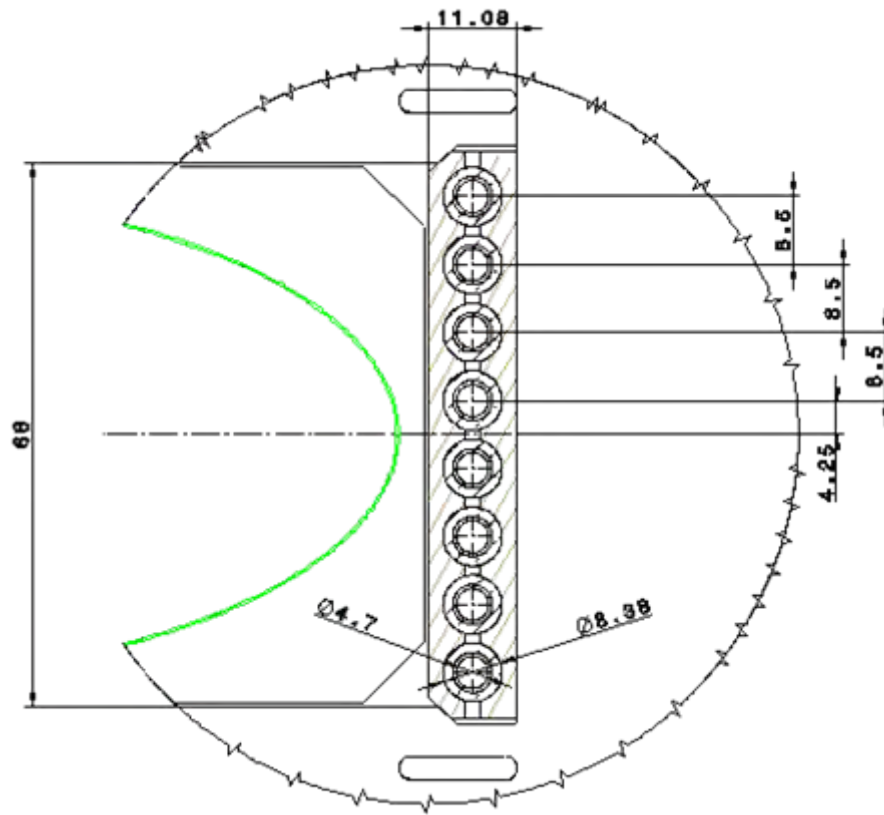
Number of strands			23	
Transposition pitch			50	mm
Cooling tube material			Cu-Ni	
Cooling tube outer diameter			5.7	mm
Cooling tube wall thickness			0.5	mm
Critical current @ 2.1 T, 4.2 K			19840	A
1st insulating layer	with epoxy impregnation			
material	Kapton	tape	2	layers
thickness/layer			50	μm
2nd insulating layer	with epoxy impregnation			
material			2	layers
thickness	Kapton	tape	70	μm
Wire				
Strand diameter			0.8	mm
Filament diameter			3.5	μm
Number of filaments			18144	
Filament twist pitch			5-8	mm
Superconducting material			NbTi	
Copper to superconductor ratio			1.5	
Copper RRR			196	
Fixation of the strands	CrNi-wire	D=0.3	transp. = 0.6	mm
Coating	epoxy compound			



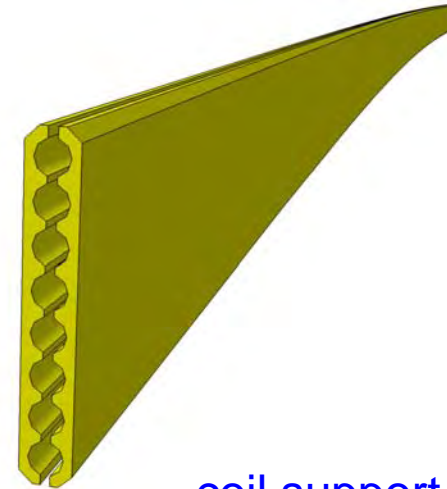
Cross section of the cable adopted for the SIS100 dipole coils (Nuclotron-type cable).

Main magnet components: Coil reinforcement

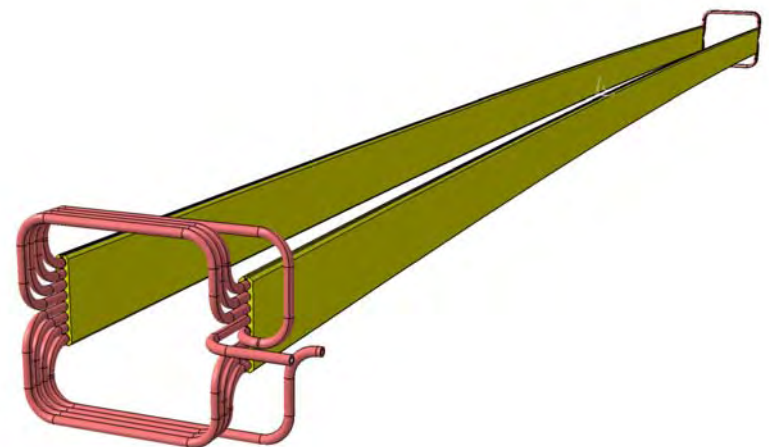
Geometric details of the dipole coil



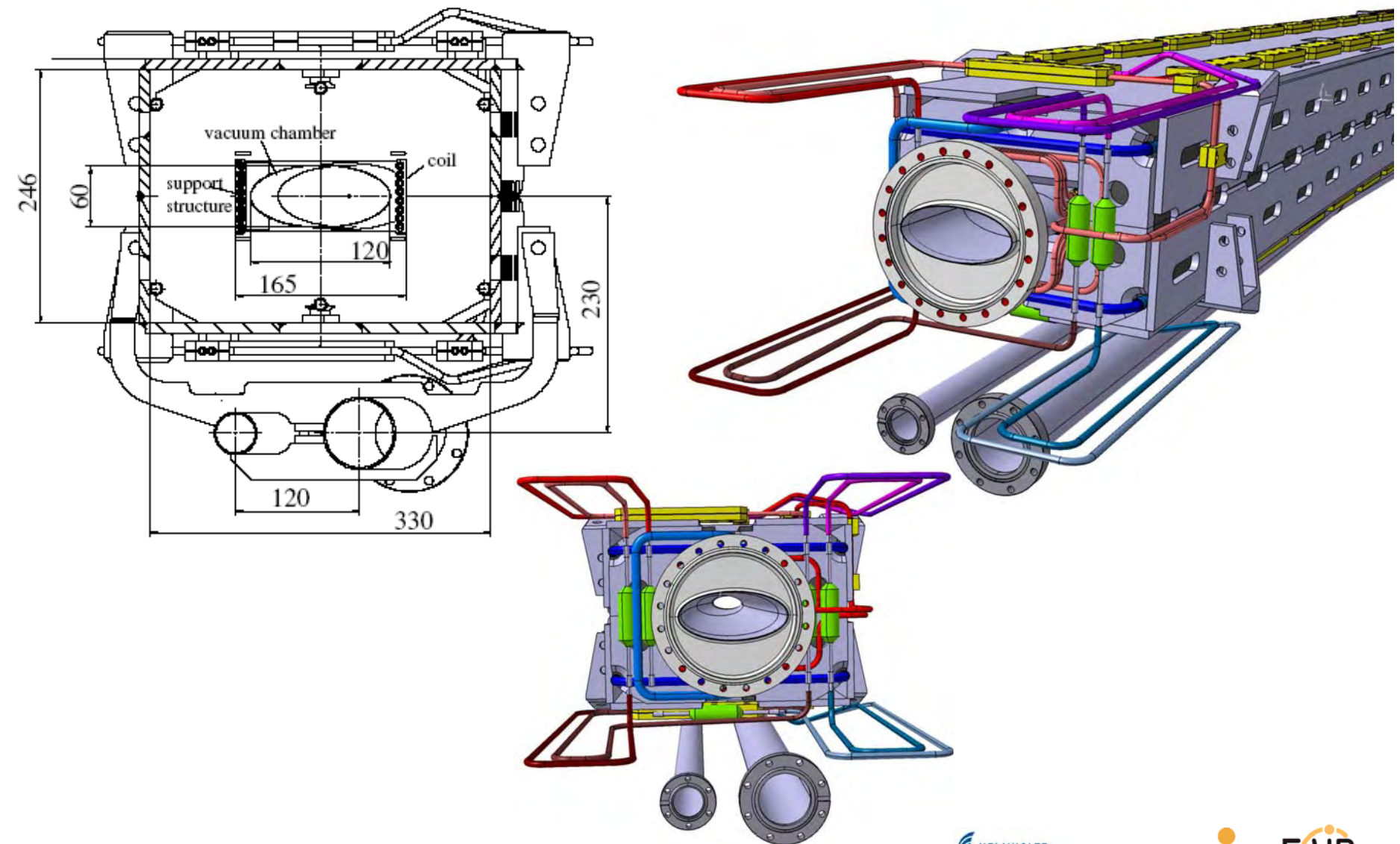
coil support structur



coil support structure
with the coil inside



Main magnet components: 3D View





1. Introduction

2. Main magnet components

- Curved single layer dipole
- **First full size magnet**

3. Mechanical stability of the coil windings

4. Magnetic steel

5. Magnetic field design

6. Losses and hydraulic limits

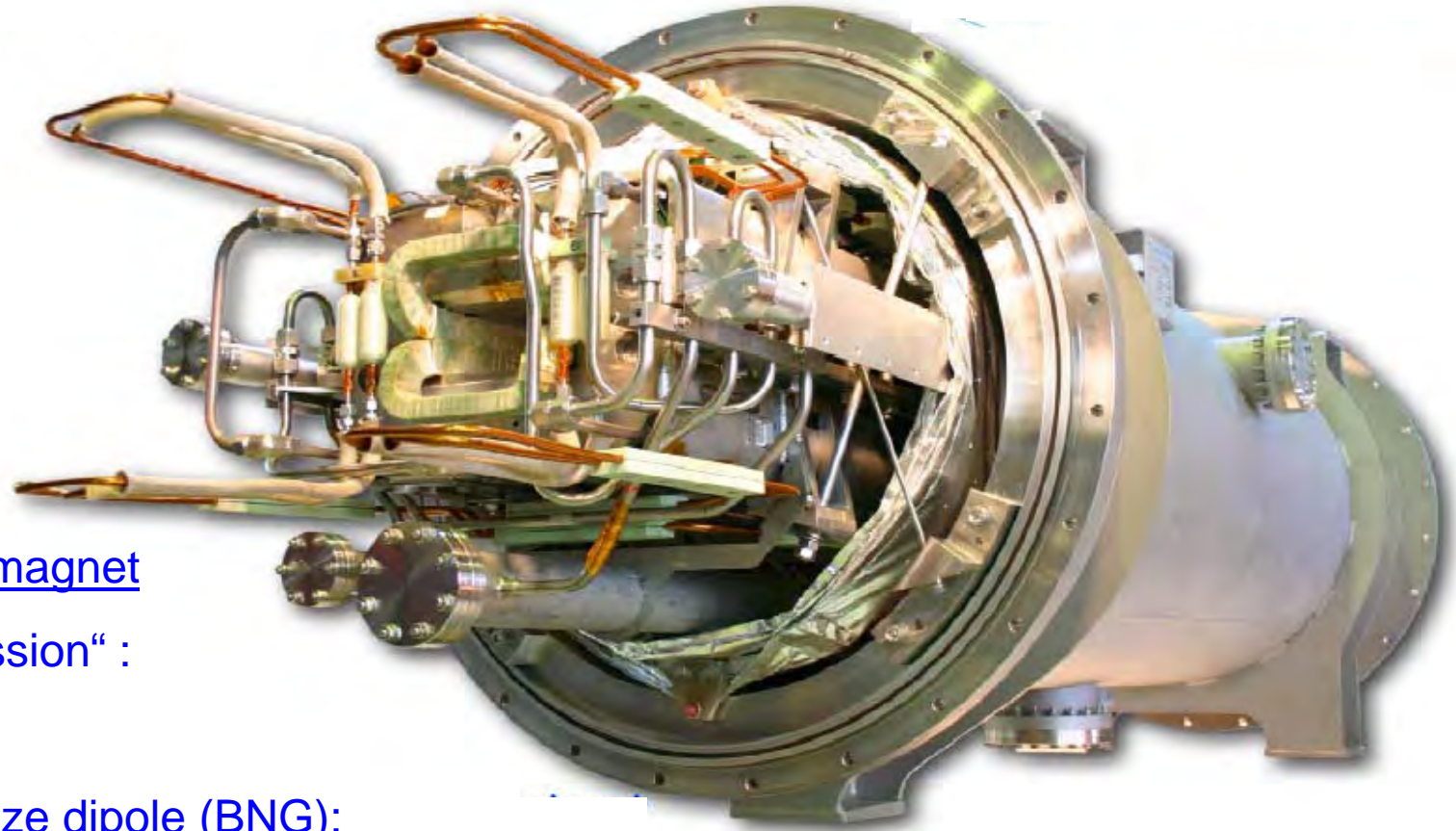
7. Vacuum chamber and temperature fields

8. Milestones towards a curved single layer dipole

9. Conclusion

Main magnet components: First full size Dipole

- Curved single layer design made
- but not yet built



- production & magnet

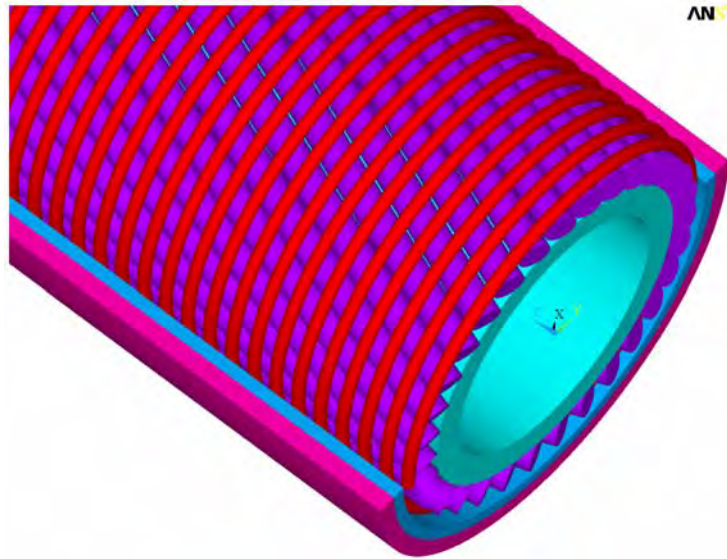
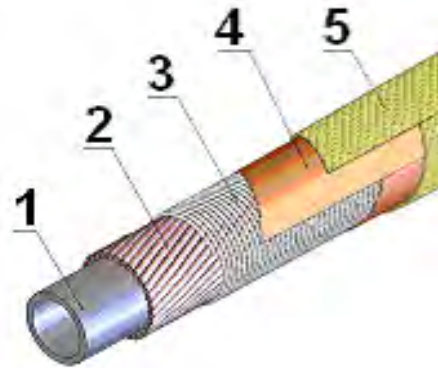
„get an impression“ :

- Nuclotron
- First full size dipole (BNG):
 - Production steps illustrated →

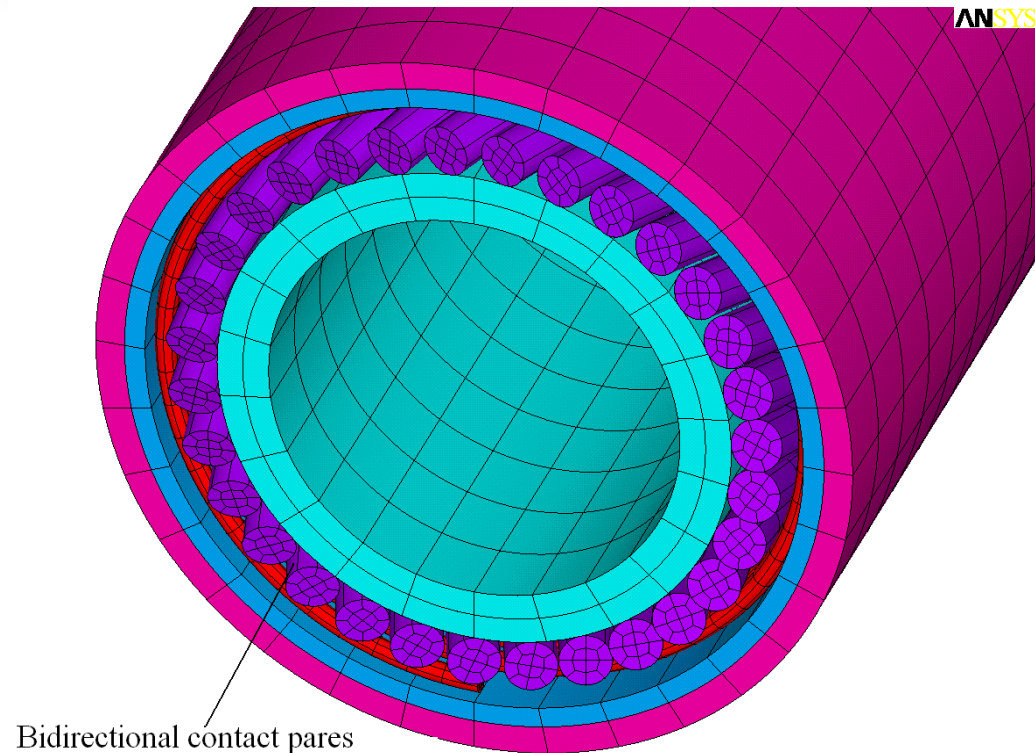
Main magnet components: Nuclotron type Cable

Nuclotron cable:

- 1 - Cooling tube CuNi
- 2 - SC wire NbTi
- 3 - CrNi wire
- 4 - Kapton tape
- 5 - Glasfiber tape



3D ANSYS modelling



SIS100 Magnets: Production of the cable

First cabling machine for the production of Nuclotron type cables



Parameters

- up to 32 wires
- "dry" and "wet" technology
- isolation with polyimide tape (2 layers)
- flexible adjustment to different cable designs (number and size of strands, size of cooling tubes, ...)

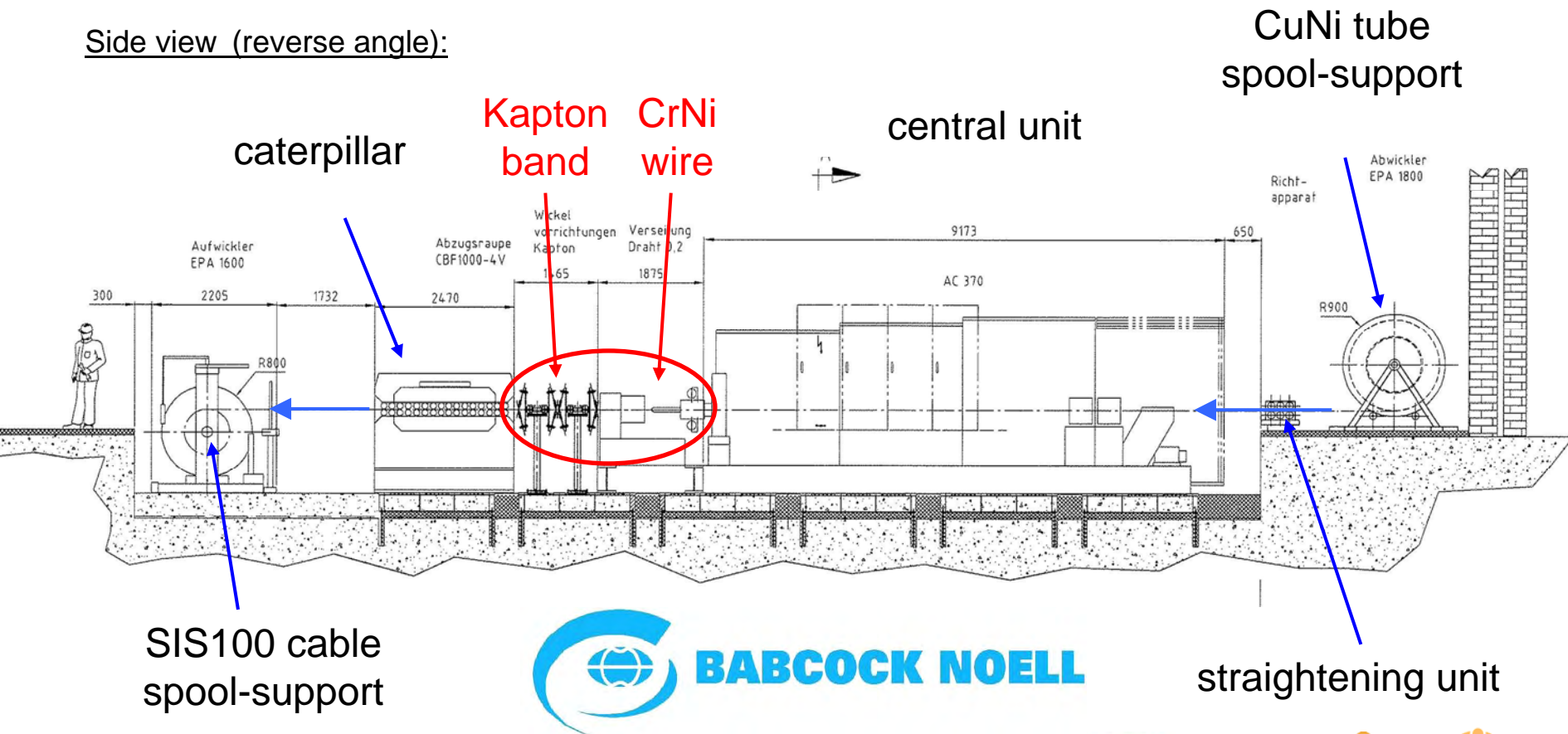
Estimated production rate: ≥ 15 m/h

Cabling facility at JINR Dubna

SIS100 Magnets: Cable machine

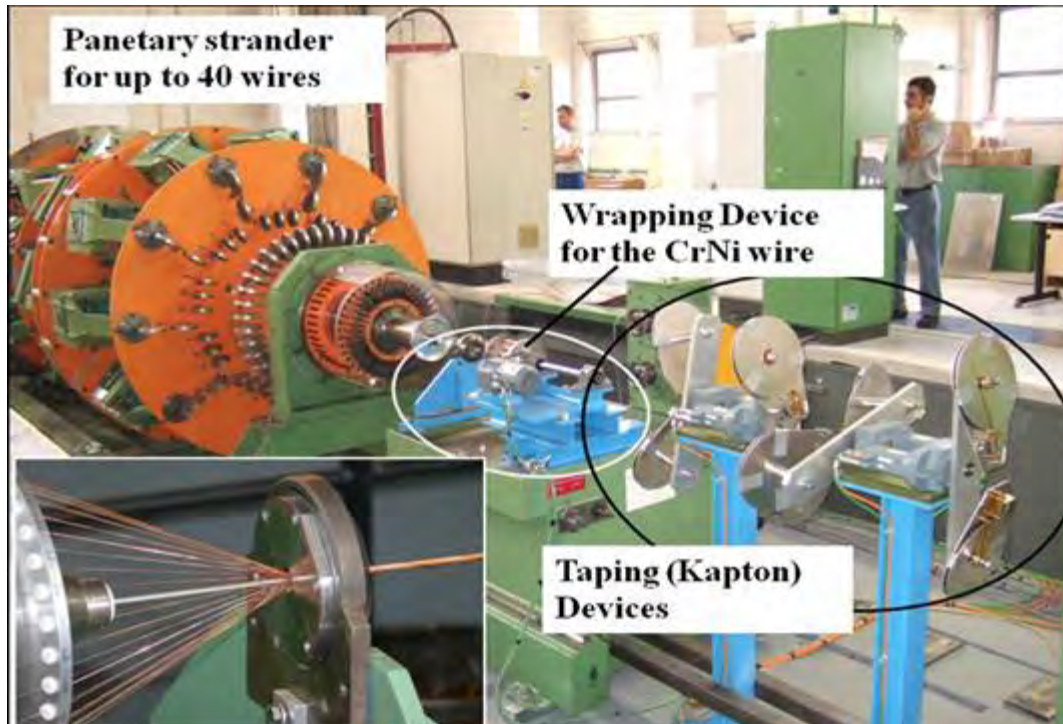
Second cabling machine for industrial production of Nuclotron type cables

Side view (reverse angle):



SIS100 Magnets: Cable production machine

Industrial cabling facility !



Cabling machine at the premises of BNG

Estimated production rate: ≥ 120 m per 8 h-shift.
 ≈ 2 complete dipole magnets

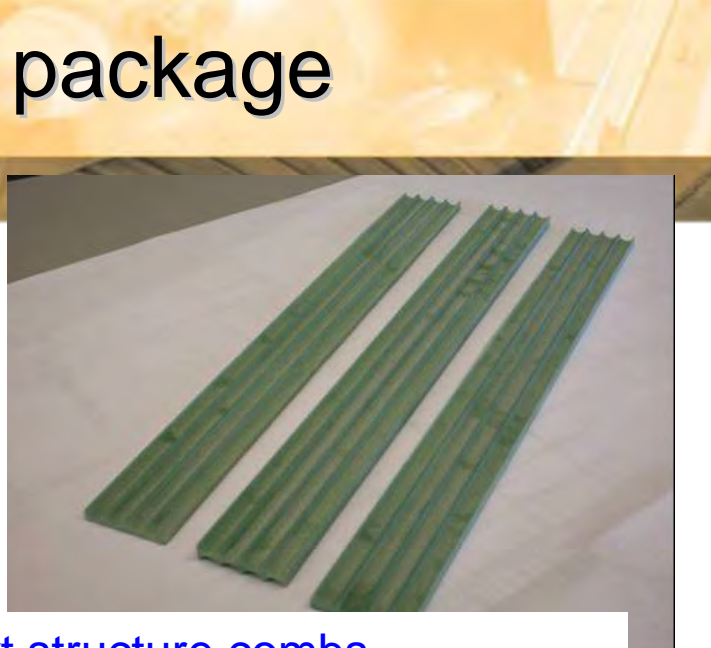
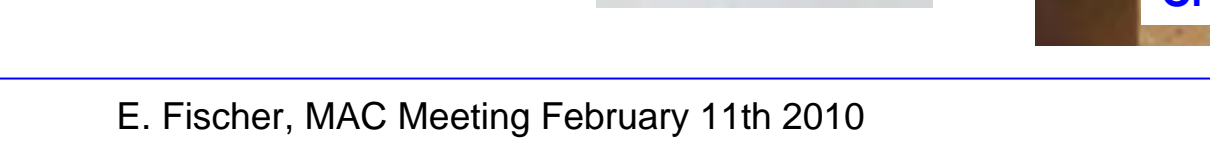
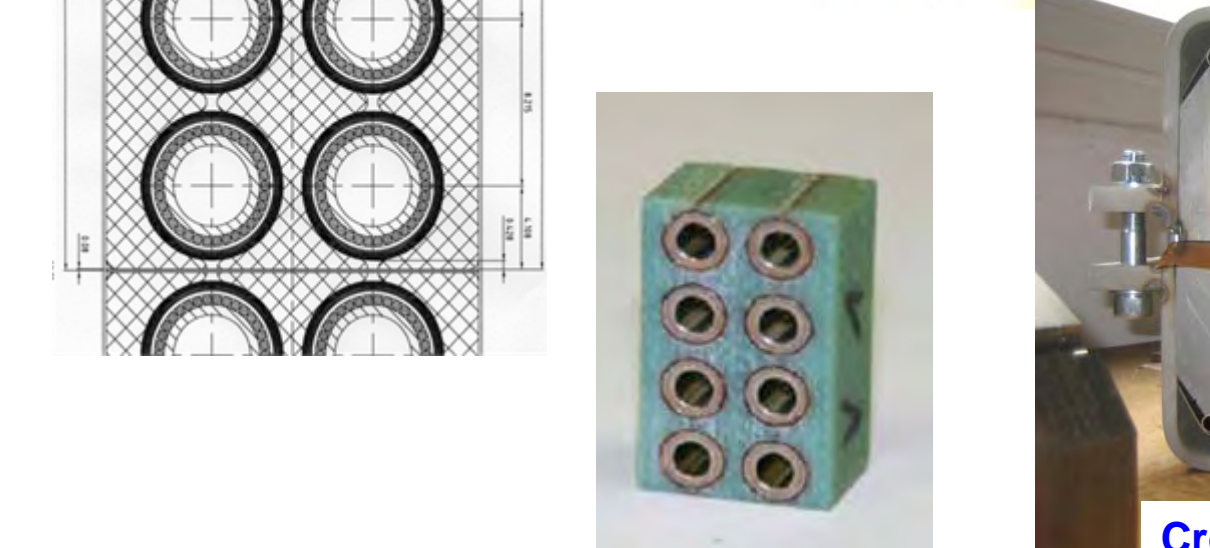
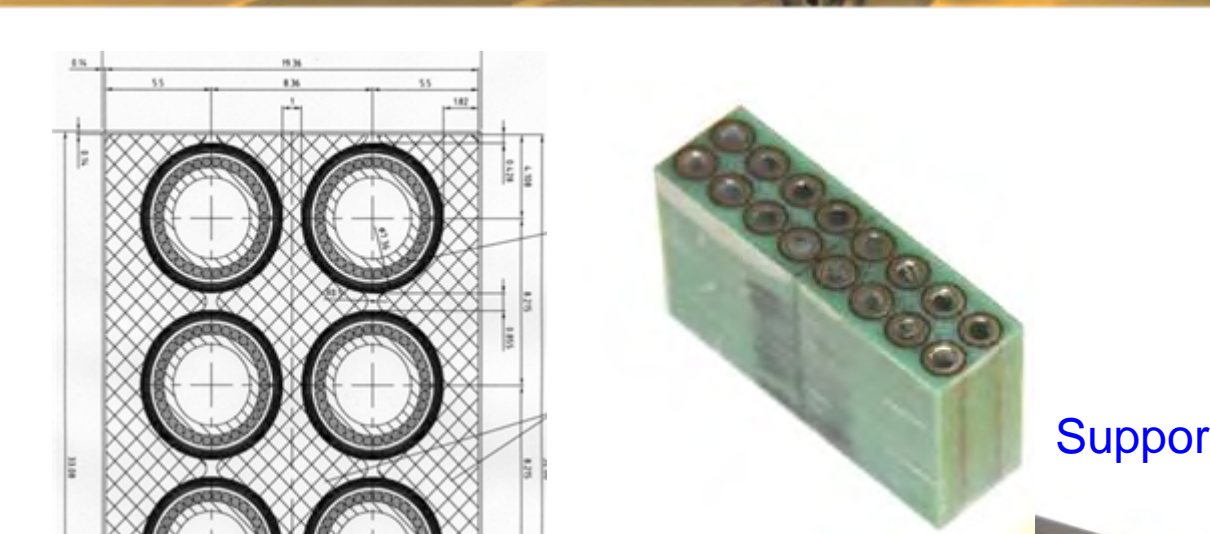
cabling facility of the BNG's :

- process safety
- reproducibility
- stable quality
- "dry" technology

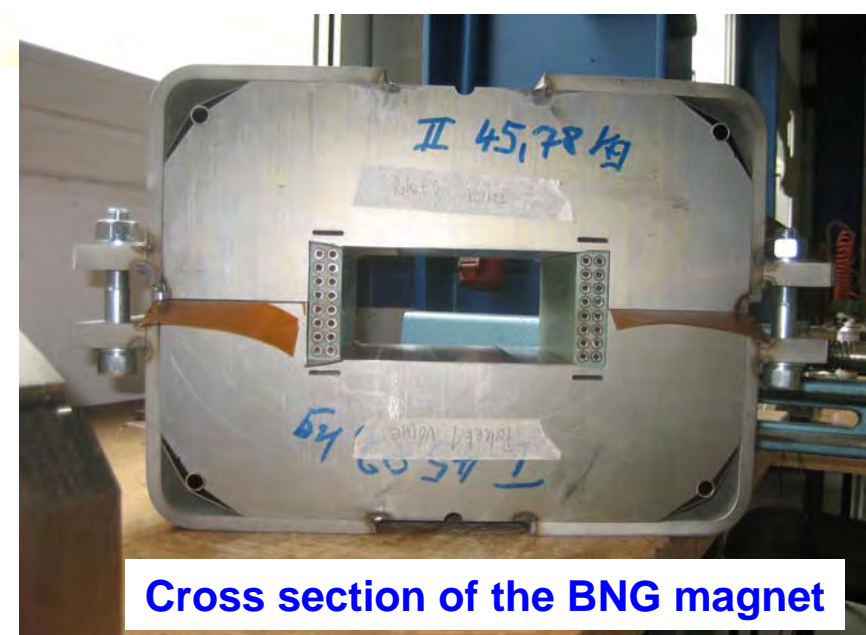
due to:

- Active and adjustable back rotation of the SC wire supply coils for all strands, avoiding torsion for all individual wires and for the cable.
- Active control of the winding force (including emergency stop) for all strands to avoid wire break and to keep winding force constant.
- Constant and adjustable torque (during operation) of CrNi wire spinning device to keep winding force of CrNi wire constant.
- Isolation with polyimide tape (up to 8 layers, with two different pitches) on-line
Flexible adjustment to different designs (number and size of strands, size of cooling tube, ...)
- All actual machine-values for winding forces, torques, speeds, and pitches can be recorded for the quality documentation.

Main magnet components: Coil package

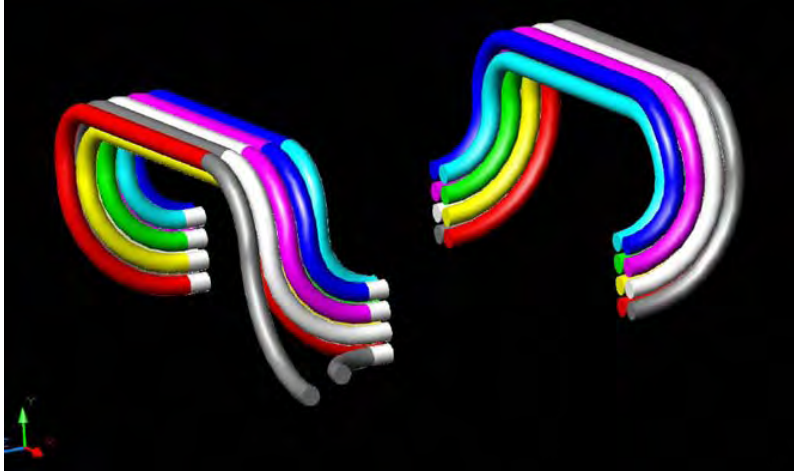


Support structure combs

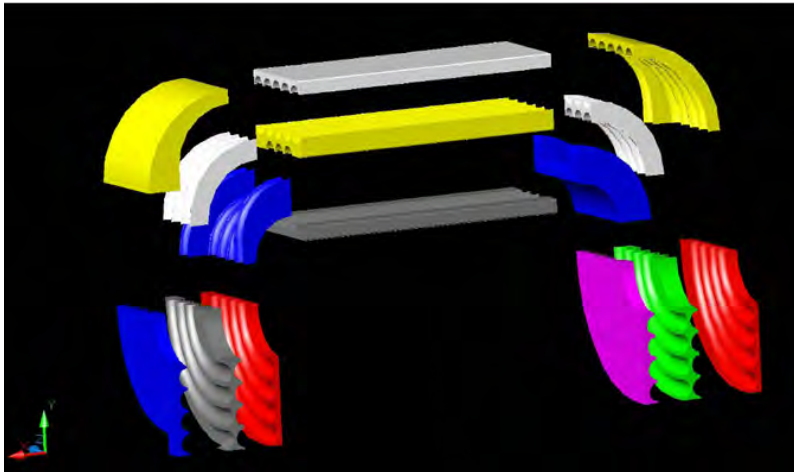


Cross section of the BNG magnet

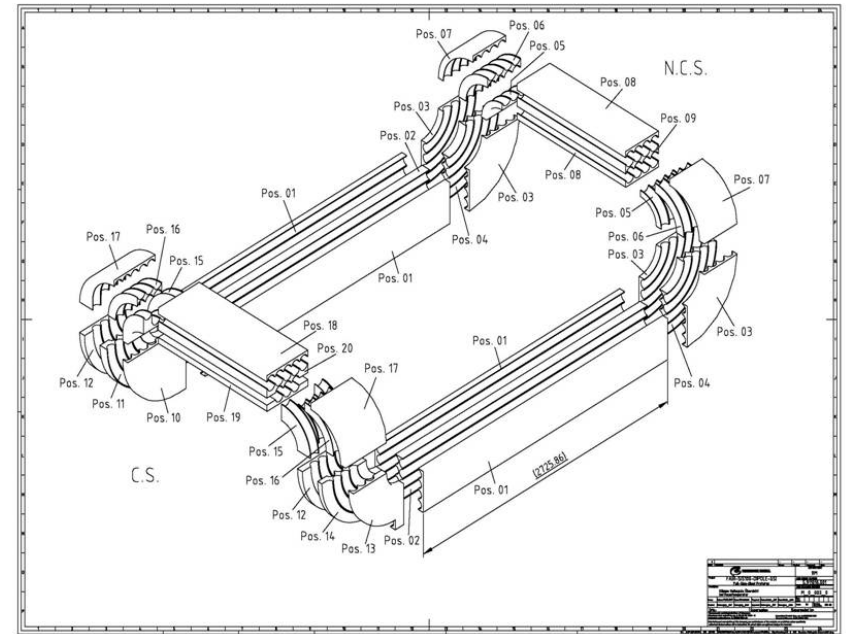
Main magnet components: Coil package



▲ layout of the coil end windings



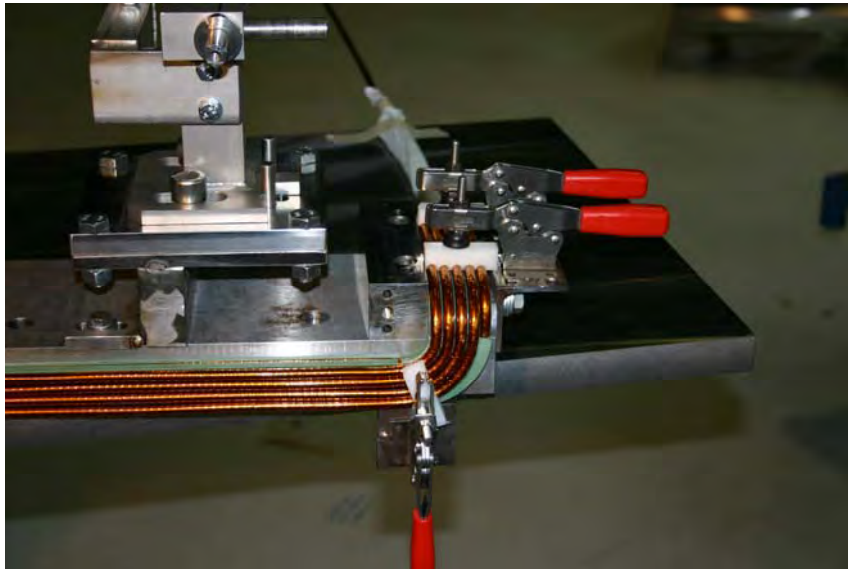
▲ reinforcement structure



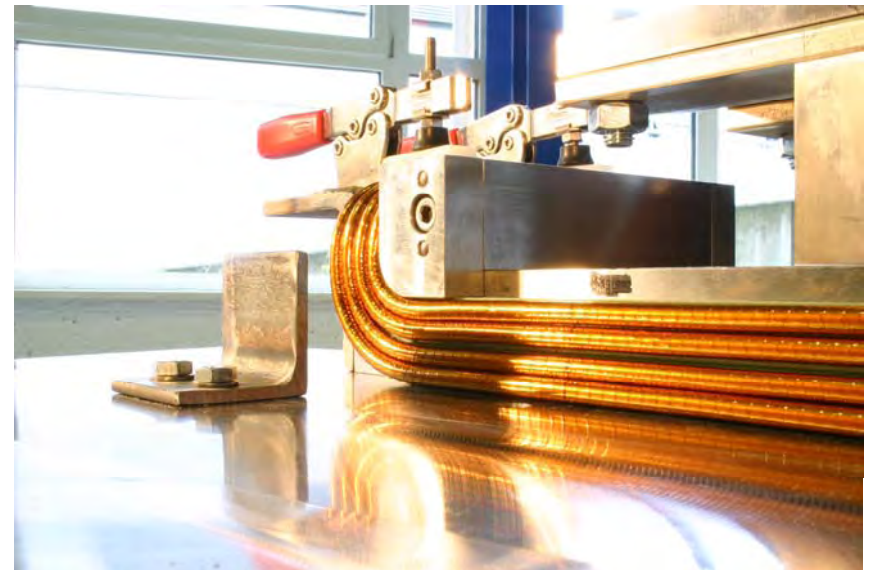
▲ coil end support drawing

Main magnet components: First full size dipole

The coil ends during fabrication at the Babcock Noell GmbH

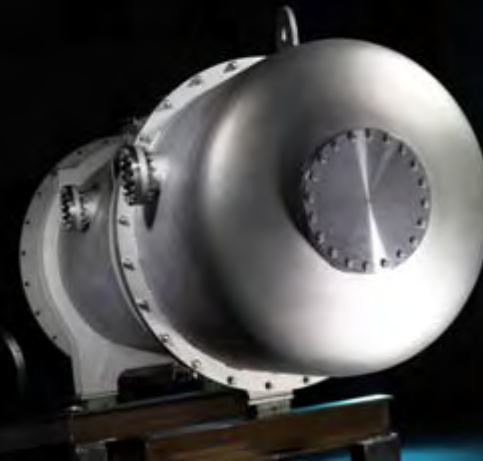
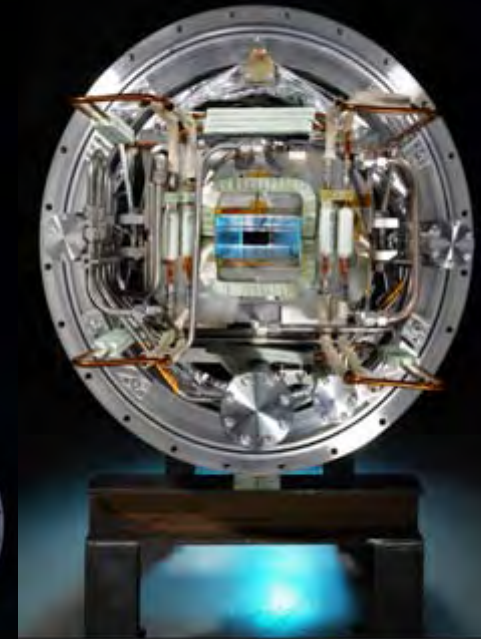
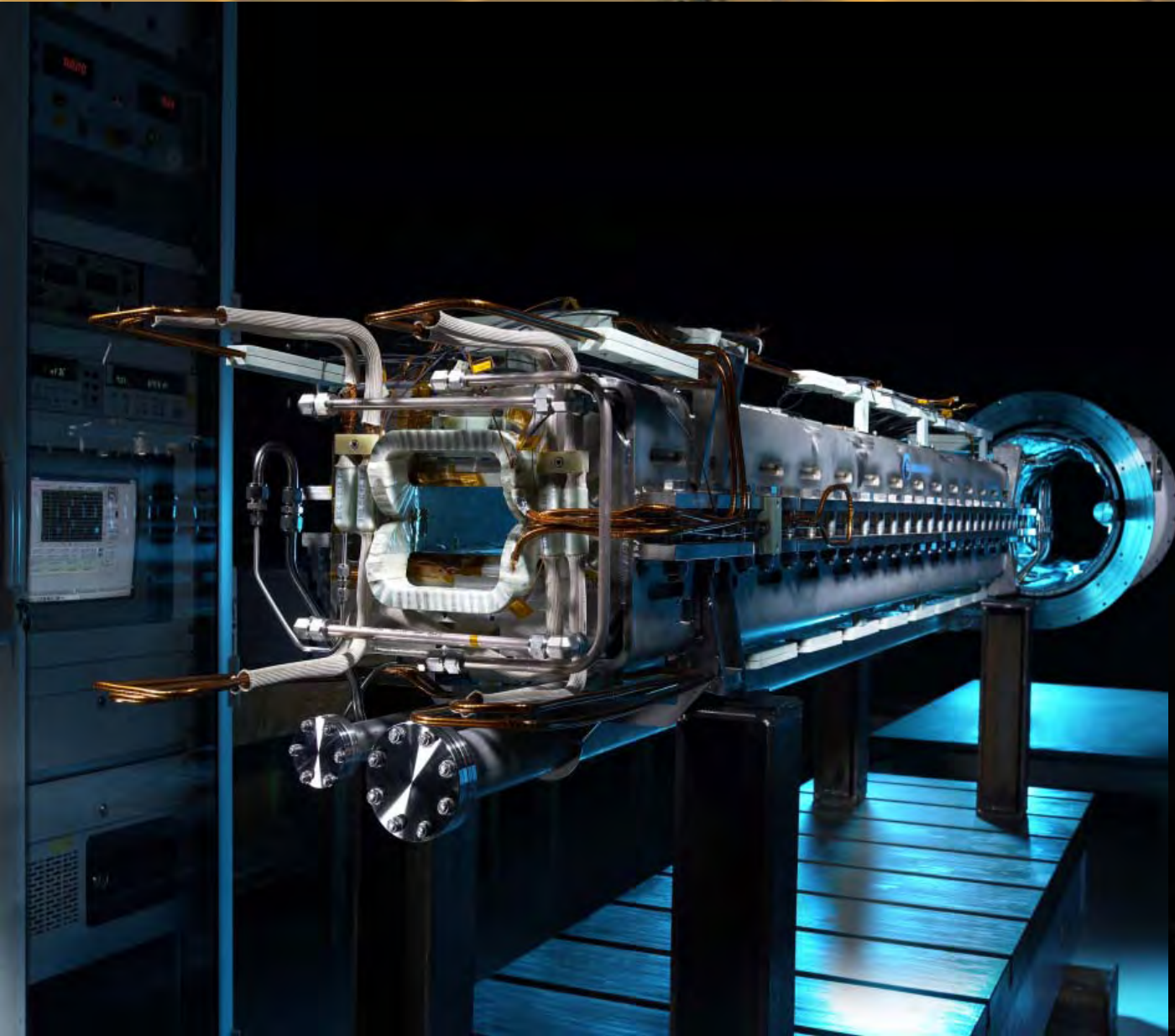



Precision of < 0.05 mm for Cable Position
and Coil Shape
+
Enhancement of Winding Pack Rigidity



Winding process. The 4th turn of the inner layer is just being pre-bent to fit into the framework created by the innermost G11 pieces. Besides the coil in progress, the winding core the (pre-) bending tooling and various clamping elements are visible.

Main magnet components: First full size dipole



- 
1. Introduction
 2. Main magnet components
 3. Mechanical stability of the coil windings
 1. Test of the cable
 2. Test of the coil pack
 3. Integral test
 4. Magnetic steel
 5. Magnetic field design
 6. Losses and hydraulic limits
 7. Vacuum chamber and temperature fields
 8. Milestones towards a curved single layer dipole
 9. Conclusion

Mechanical stability: Tests

Goal:

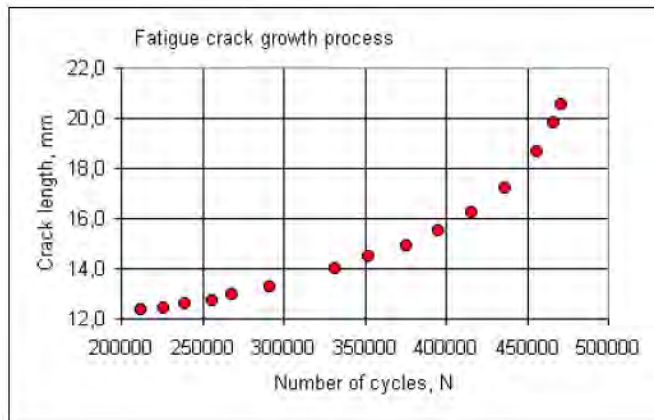
- Survival of the Cu-Ni- tube for at least 20 years of operation
- Stable coil package
- Technological optimization for production process of the cable

Tests of the mechanical properties of parts of cable and coil (at FZ Karlsruhe):

- fatigue crack growth rate of the CuNi material
- thermal expansion coefficients
- tensile strength at 4K and 300K
- leak test after mechanical load
- G11 material of the coil support structure modulus in different directions
- stress-strain curves before and after 2 million cycles
- leak test before and after 3 million cycles
- thermal expansion coefficients and leak test before and after thermal cycles
- stress-strain-curve after thermal cycling

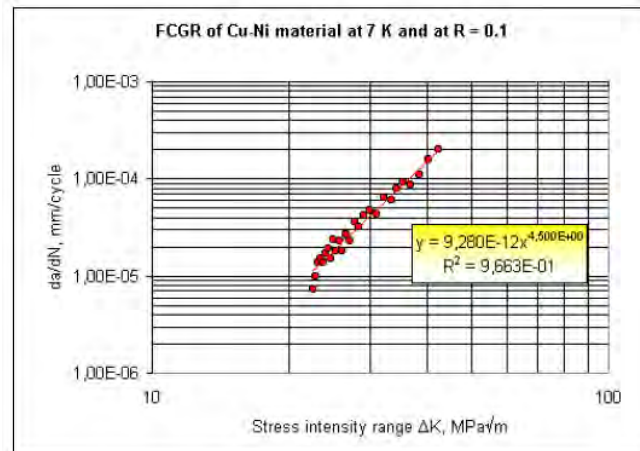
Mechanical stability: Crack growth in CuNi tube

Measurements of the fatigue crack growth rate on CuNi material at FZ Karlsruhe:



$$a_0 = d/2 = 0.1 \text{ mm}$$

$$a_f = \frac{1}{\pi} \left(\frac{KIC}{\Delta\sigma YS} \right)^2$$



Integration of Paris law:

$$N_f = \int_{a_0}^{a_f} \frac{1}{C (YS\Delta\sigma\sqrt{\pi a})^m} da \approx 250 \cdot 10^6$$

➤ Under the given conditions the tube will sustain more than 250 million cycles.

Mechanical Stability: CuNi tube – stress strain

stress-strain measurements on the CuNi tube
for different treated samples:

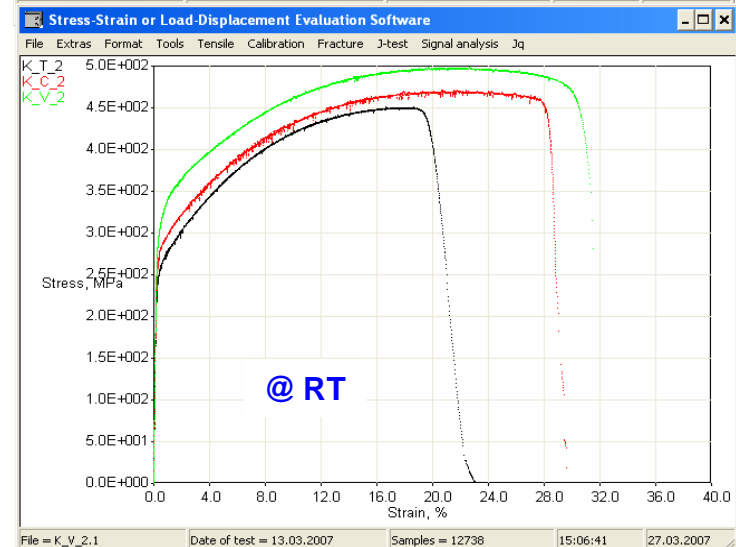
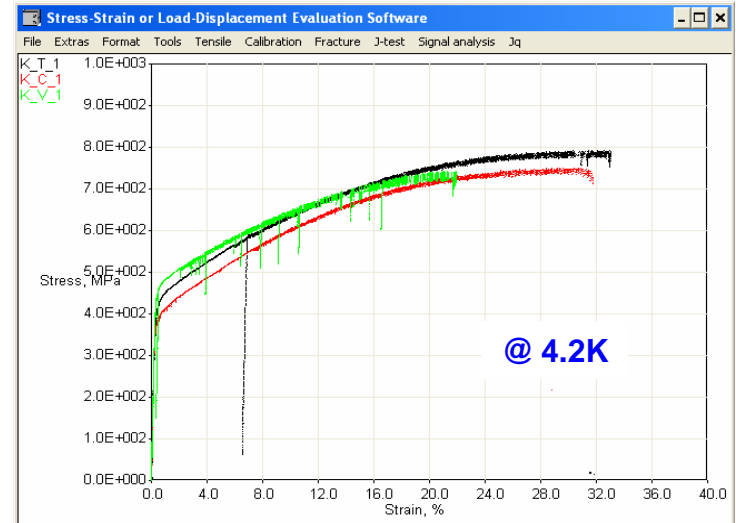
K_t: annealed in Argon gas

K_c: after 100 rapidly thermal cycles (80 – 300K)

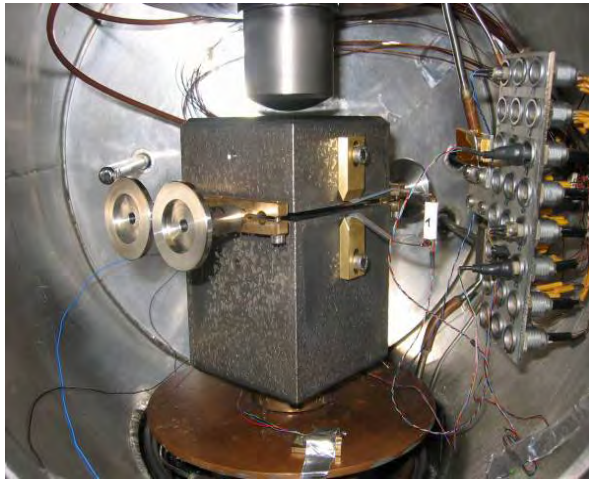
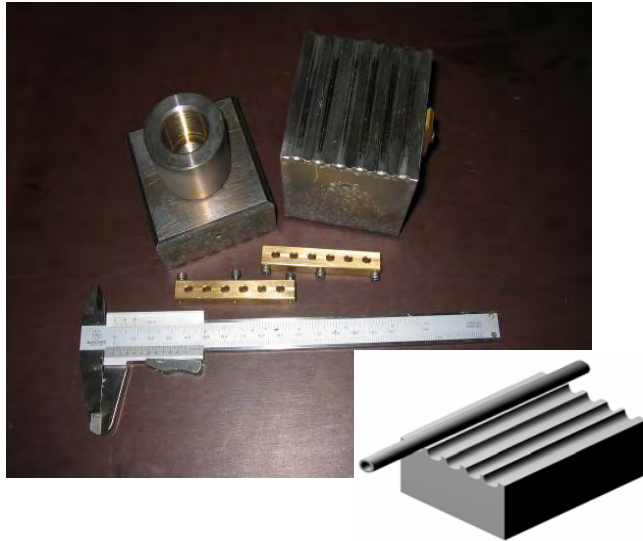
K_v: annealed + 100 thermal cycles



File	T K	E- Modulus GPa	Yield Strength MPa	Ultimate Tensile Strength MPa	Uniform Elongation %	Total Elongation %
K _t 1	4.2	163	414	792	32,1	33,1
K _t 2	RT	165	250	451	18,6	23,1
K _c 1	4.2	156	385	751	28,8	31,6
K _c 2	RT	154	274	471	21,8	29,9
K _v 1	4.2	161	379	743	21,0	21,9
K _v 2	RT	155	300	498	19,7	32,2



Mechanical Tests: CuNi tube – leak tests



Mechanical test of the CuNi tube

load	leak rate test for cycling with $F_{\max} = 800 \text{ N}$ and $T < 7 \text{ K}$	
	before cycling	after $2,6 \times 10^6$ cycles
sample nr.	LR. mbarl/s	LR. mbarl/s
1	$1,3 \times 10^{-9}$	$1,2 \times 10^{-9}$
2	$1,7 \times 10^{-9}$	$2,1 \times 10^{-9}$
3	$9,2 \times 10^{-8}$	$2,8 \times 10^{-9}$
4	$1,5 \times 10^{-9}$	$1,5 \times 10^{-9}$
5	$3,3 \times 10^{-9}$	6×10^{-9}
6	$2,8 \times 10^{-9}$	$3,2 \times 10^{-9}$

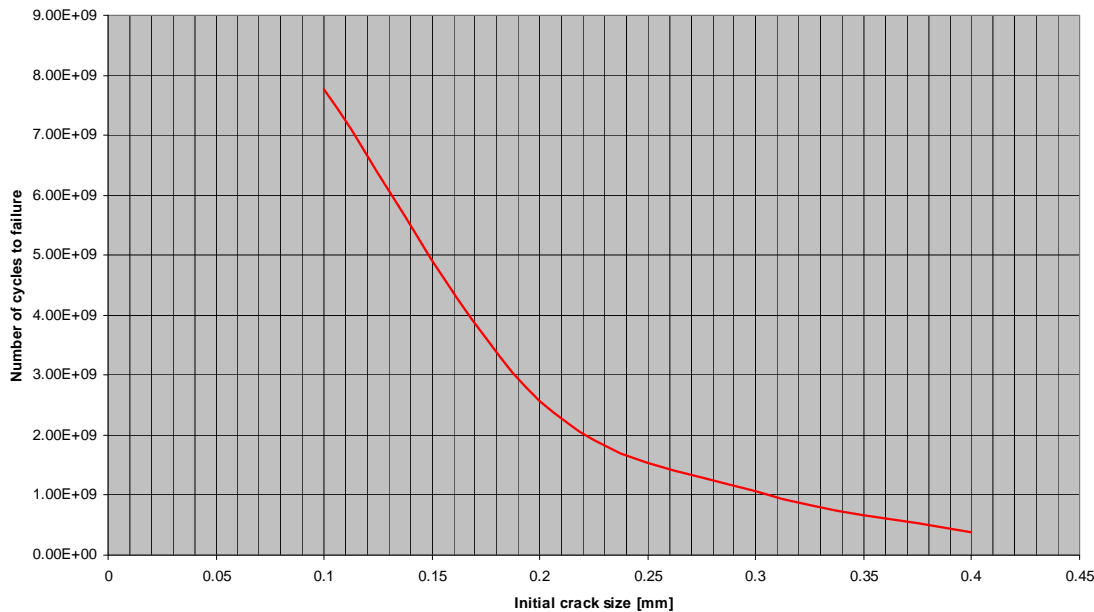


➤ the mechanical cycling test had shown no impact on the leak rate for the CuNi tube of the SC-cable !

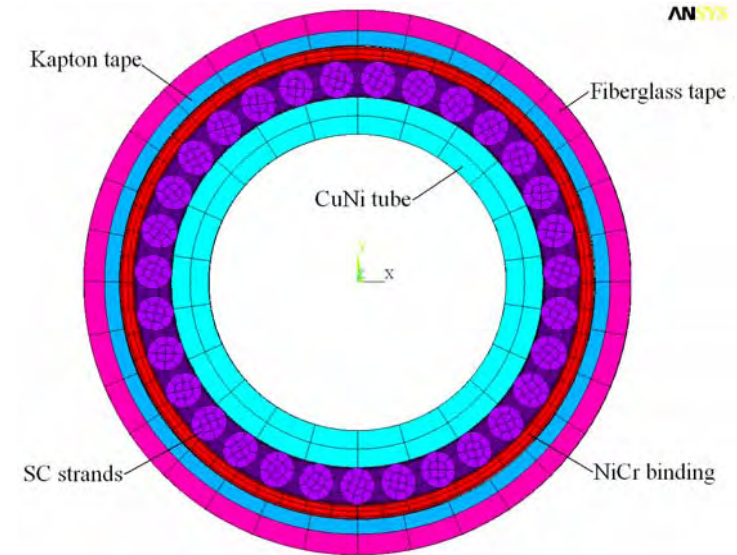
Mechanics: Cable -- FEM Analysis

ANSYS calculations for fatigue behaviour and structural integrity:

NUMBER OF CYCLES TO FAILURE OF THE CuNi TUBE AS A FUNCTION OF INITIAL CRACK SIZE



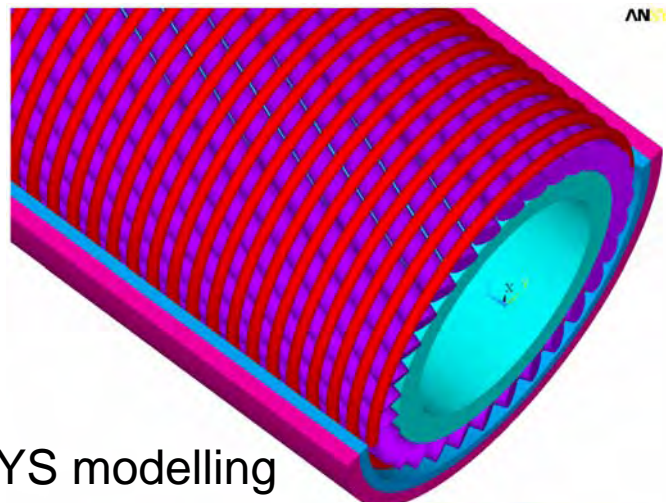
- no fatigue problems
- no crack propagation problem
- tube will survive 20 years of operation



Detailed and physical accurate FEM modeling of the cable, also for further investigations

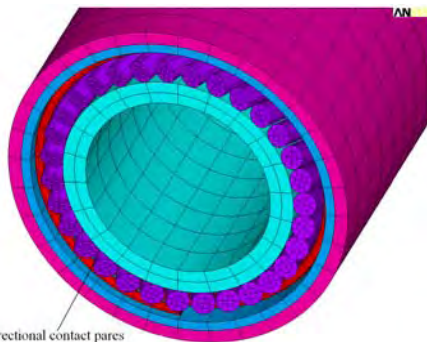
Mechanics: Cable - FEM Analysis

- study of structural integrity of the cable
- analysis of the thermo-mechanical properties
- impact of the load cycles on the coil pack $> 2 \cdot 10^8$ cycles

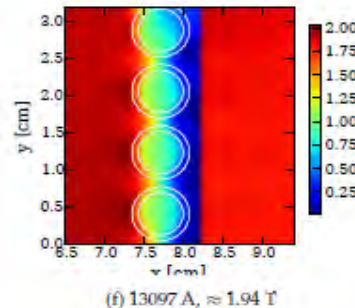


ANSYS

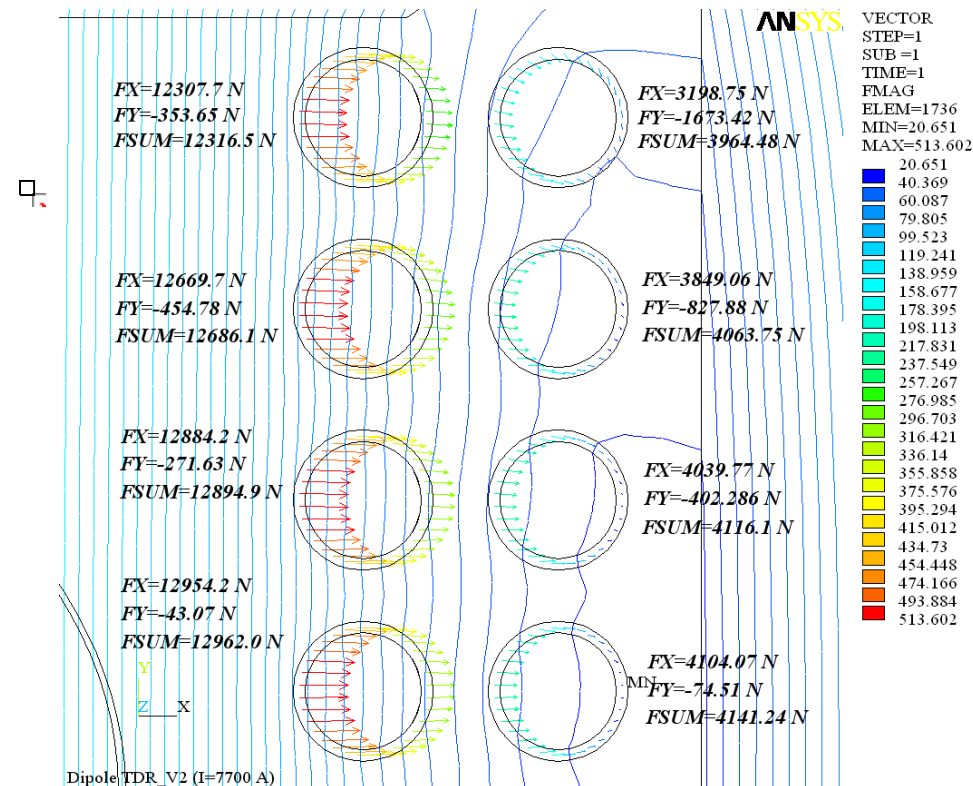
3D ANSYS modelling




Bidirectional contact pairs



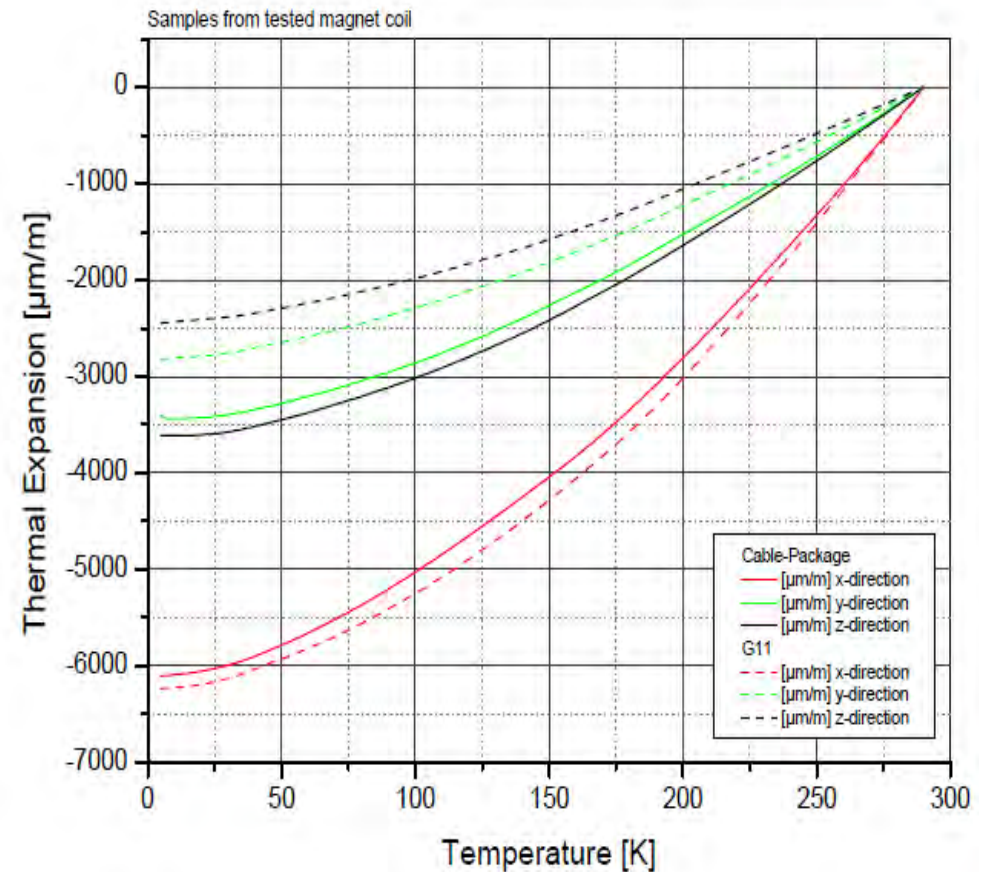
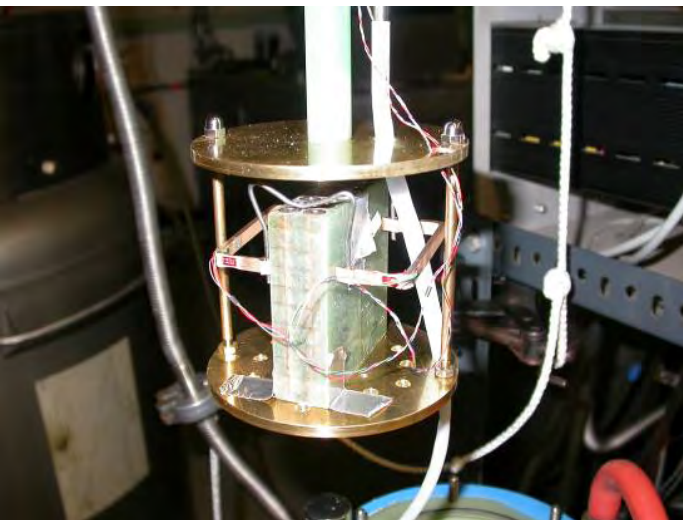
field distribution $\mathbf{B}(x,y)$



- 
1. Introduction
 2. Main magnet components
 3. Mechanical stability of the coil windings
 1. Test of the cable
 2. Test of the coil pack
 3. Integral test
 4. Magnetic steel
 5. Magnetic field design
 6. Losses and hydraulic limits
 7. Vacuum chamber and temperature fields
 8. Milestones towards a curved single layer dipole
 9. Conclusion

Coil package: thermal expansion

Test of the support structure material



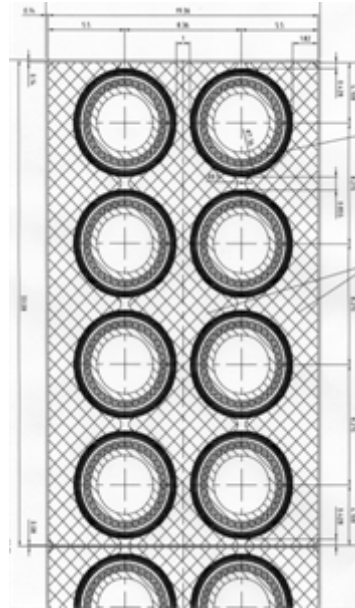
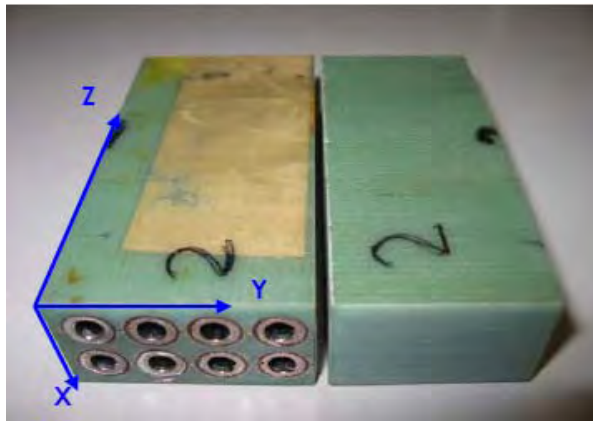
▲ Measurement result of the thermal contraction for the coil pack

▲ Thermal expansion measurements

Coil package tests: Interlamination shear

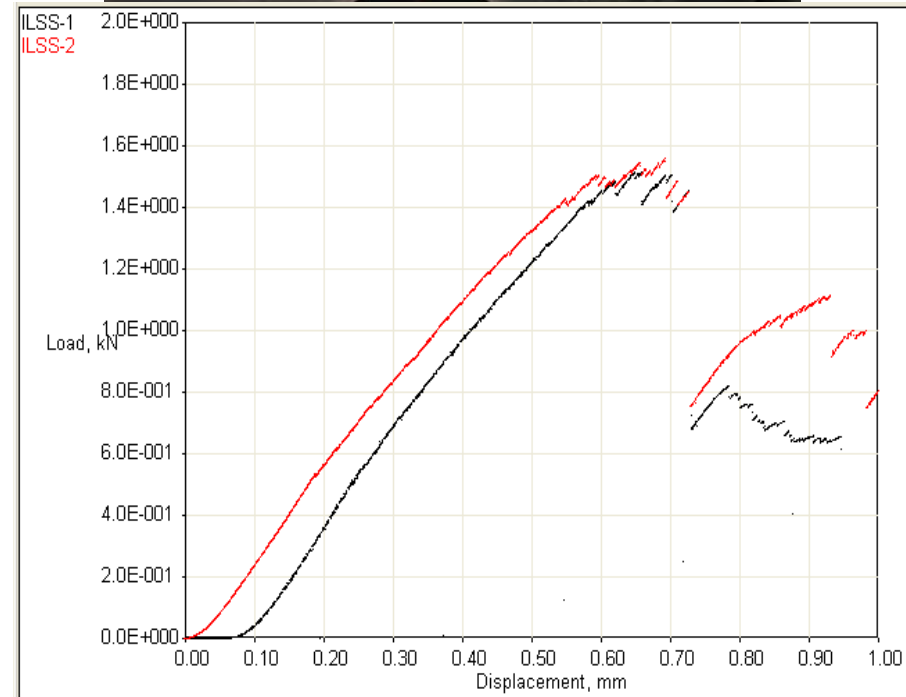
Coil support structure:

- reduction of point loads
- accurate positioning



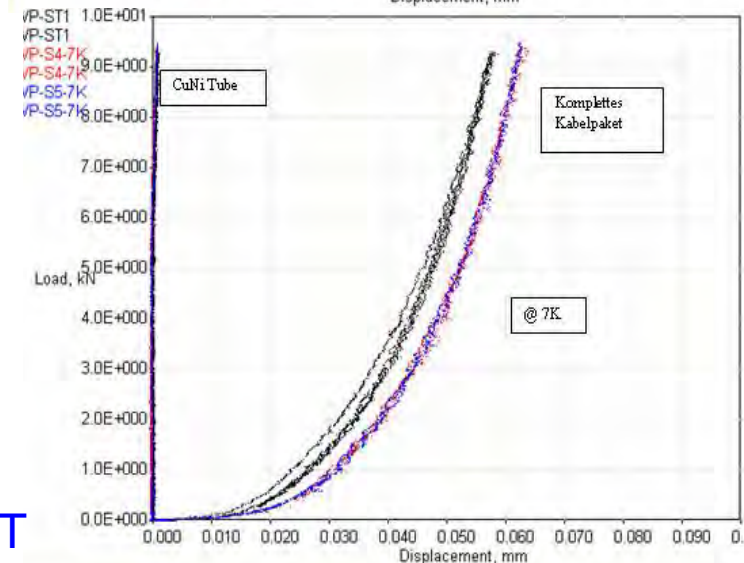
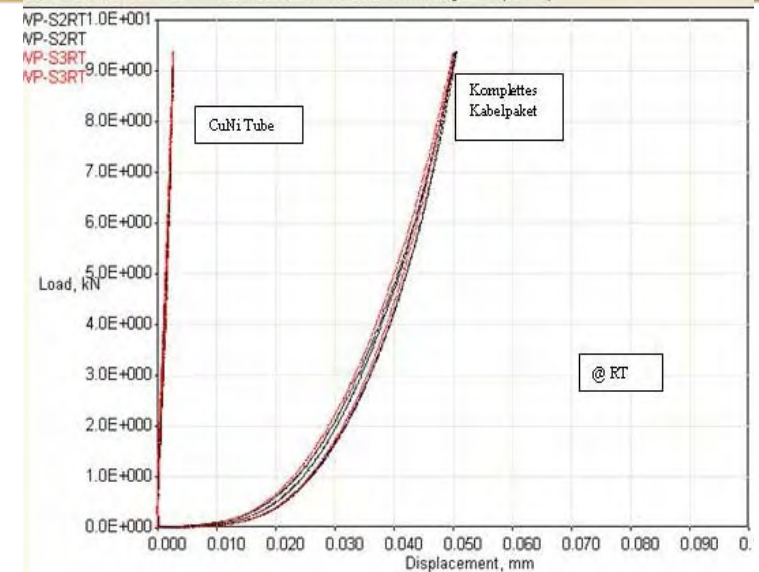
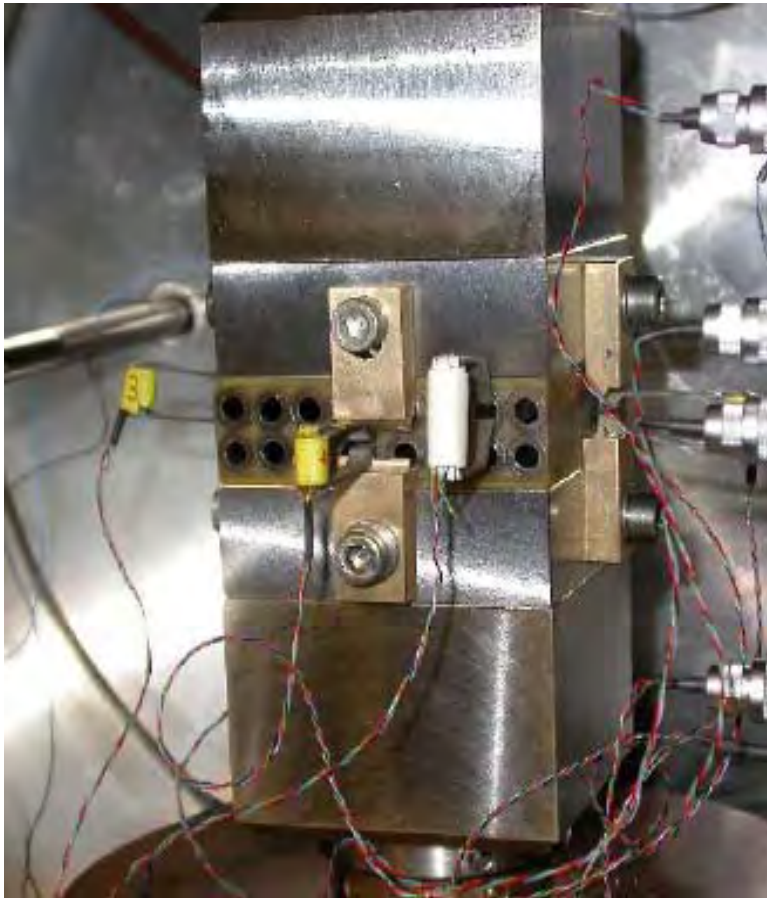
- **mechanical measurements of the coil support structures textured material G11**

G11 Sample	T K	Stiffness N/mm	E Modul GPa	Fmax N	ILSS MPa
Sample 1	7	162,8	32,9	1,515	57,8
Sample 2	7	163,9	33,1	1,559	59,1



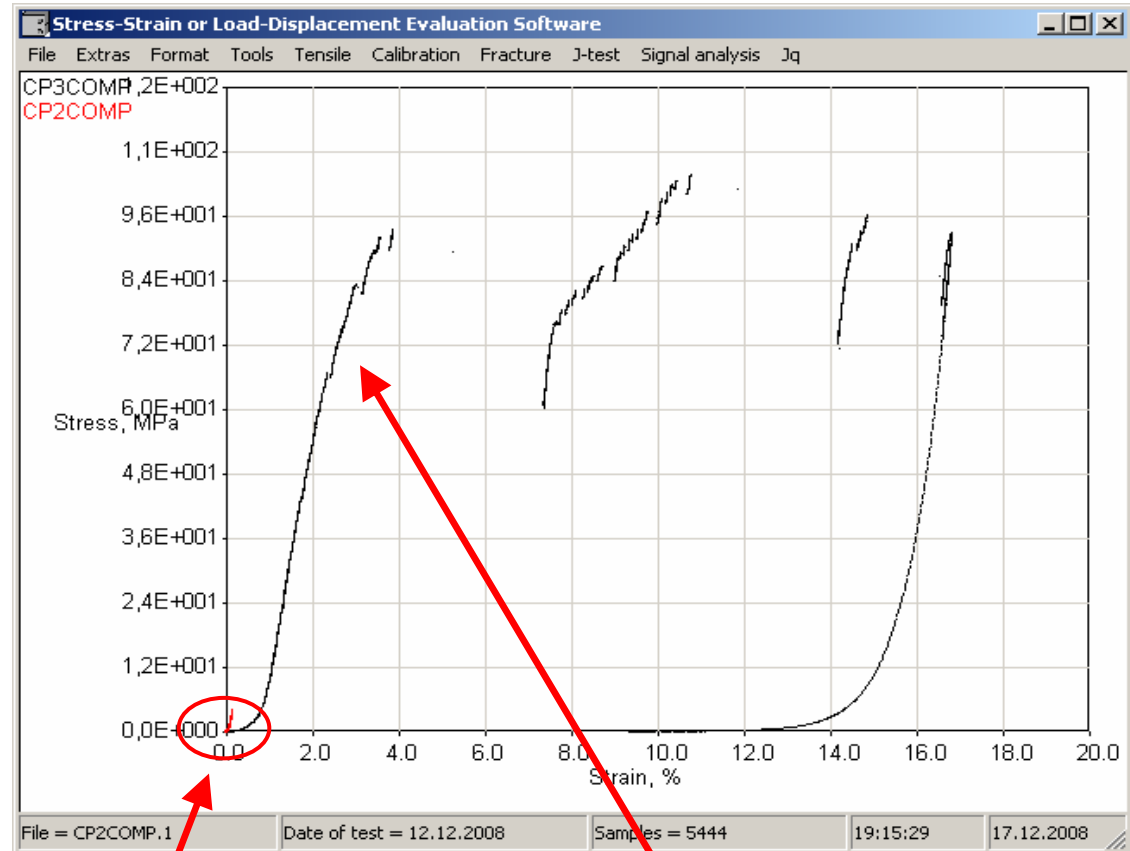
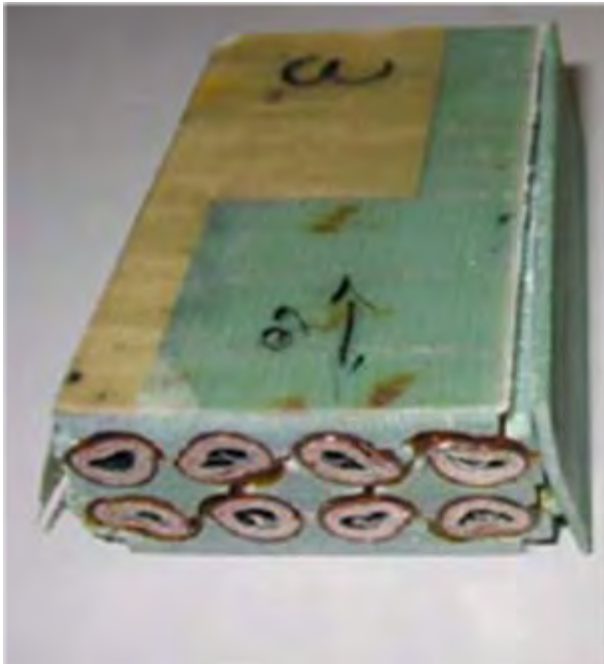
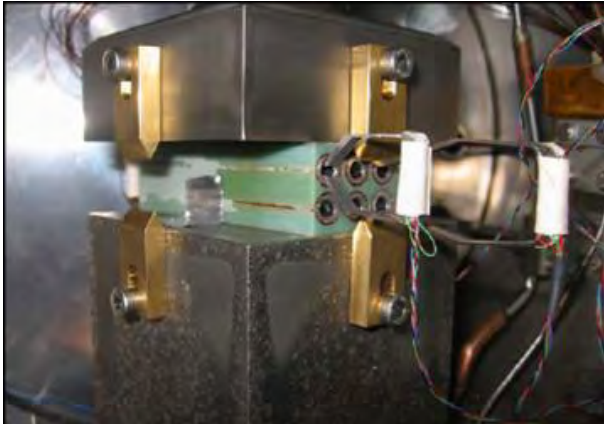
Coil package: stiffness @ RT, 7K

- Measurement of the coil pack stiffness at room temperature and at 7 K.




movement of the coil windings $< 5 \mu\text{m}$ at $B_{\text{max}} = 2 \text{ T}$

Coil package tests: cycling - destruction



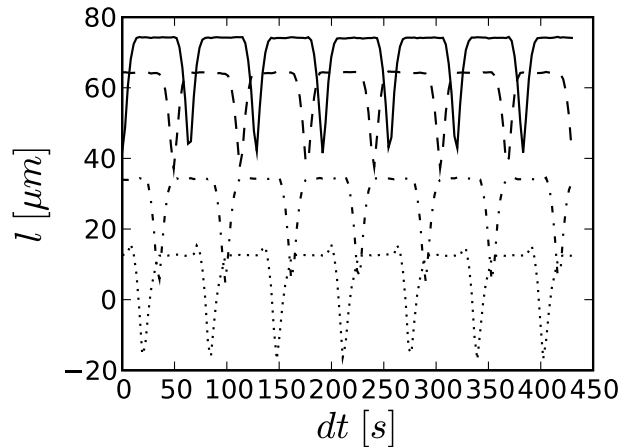
load cycles

destruction

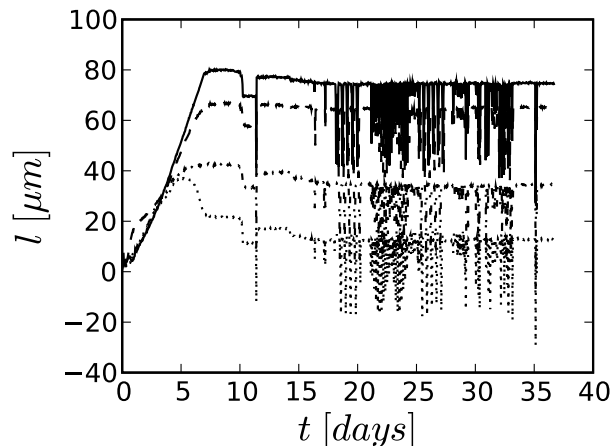
- 
1. Introduction
 2. Main magnet components
 3. Mechanical stability of the coil windings
 1. Test of the cable
 2. Test of the coil pack
 3. Integral test
 4. Magnetic steel
 5. Magnetic field design
 6. Losses and hydraulic limits
 7. Vacuum chamber and temperature fields
 8. Milestones towards a curved single layer dipole
 9. Conclusion

Mechanics: Integral test

The movement of the coil versus the yoke



▲ while cycling the magnet



▲ during cool down and cycling

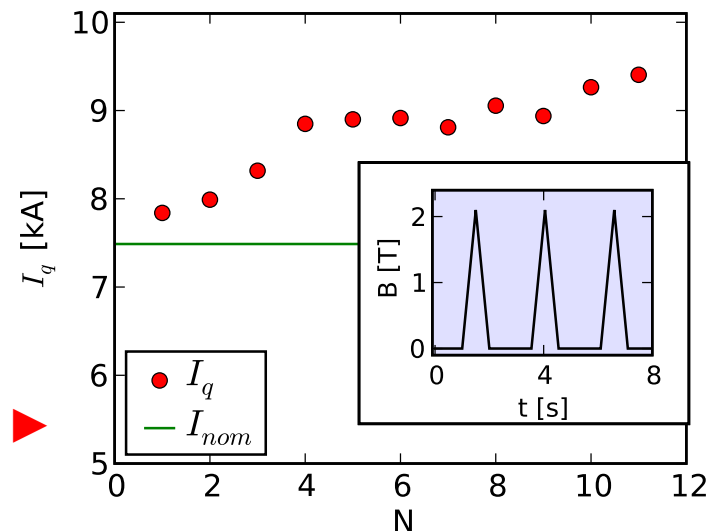



DC Quench training ►

cycling tests



inset on the right:
the strongest cycle mode of the
magnet continuously tested
during one week and up to now
for $5 \cdot 10^5$ cycles.



- 
1. Introduction
 2. Main magnet components
 3. Mechanical stability of the coil windings
 4. **Magnetic steel**
 - Dependence on Si content
 - Steel Comparison
 - Selection
 5. Magnetic field design
 6. Losses and hydraulic limits
 7. Vacuum chamber and temperature fields
 8. Milestones towards a curved single layer dipole
 9. Conclusion

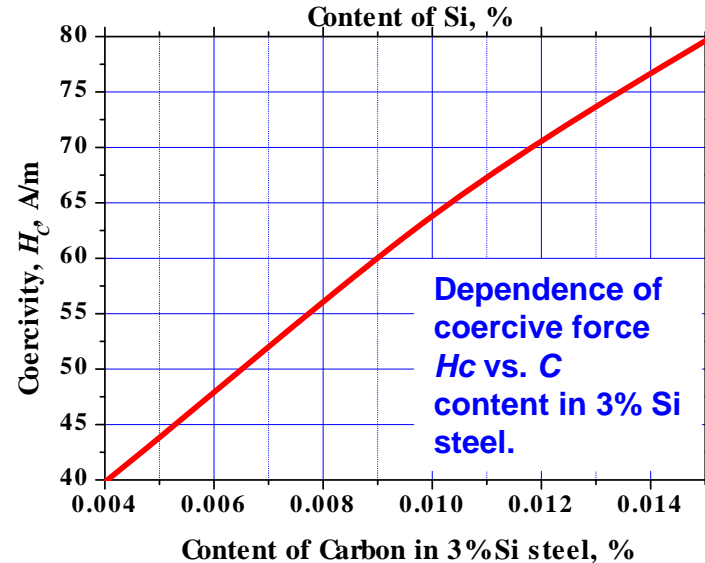
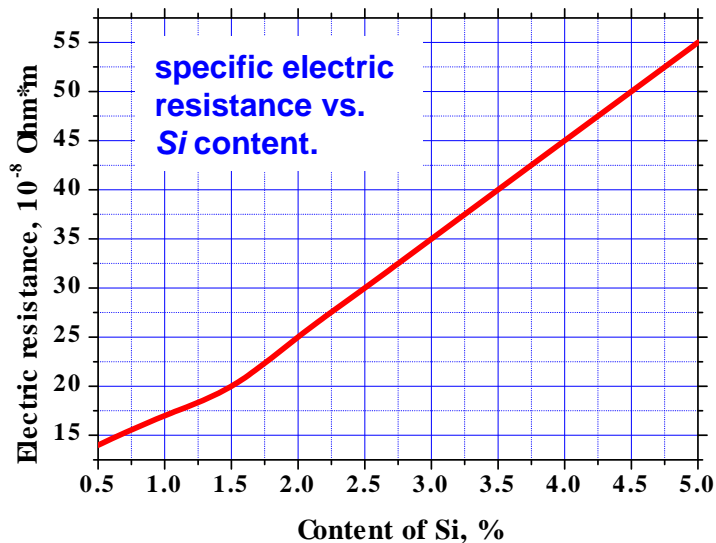
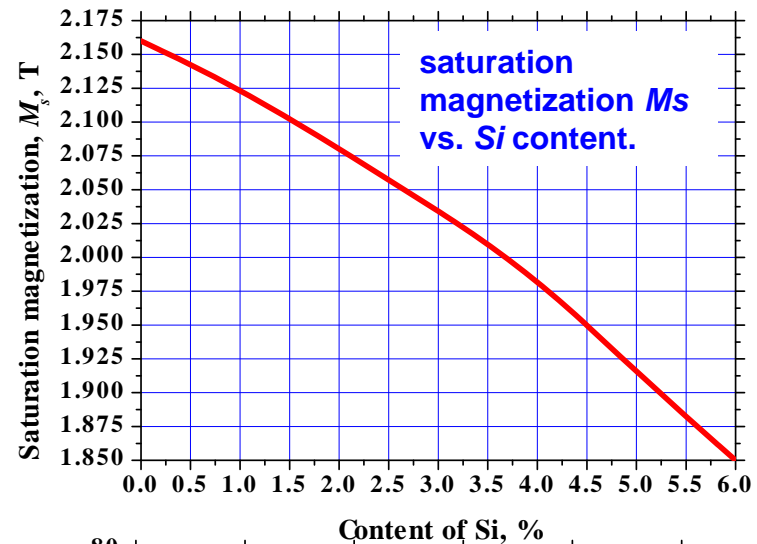
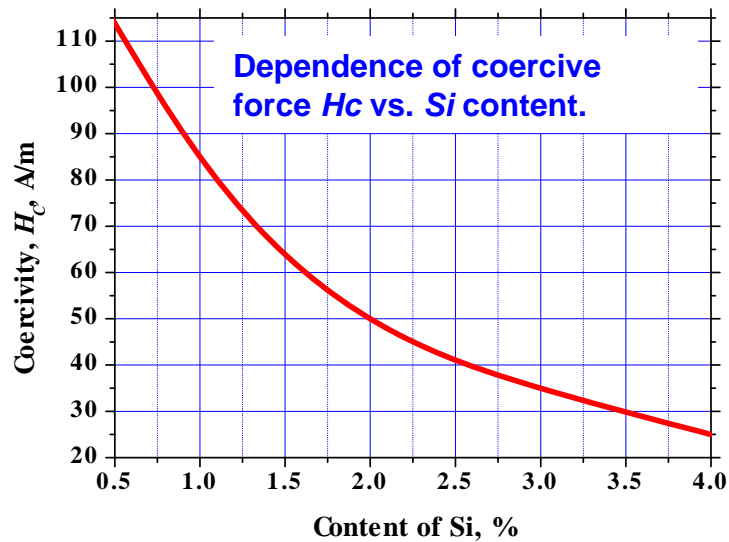
Magnetic steel

The choice of the electrical steel, best appropriate for the operation parameters of the main SIS100 magnets, is crucial for an optimal adjustment of the requirements to achieve high field quality, minimum AC losses in the yoke and a safe, reproducible production technology.

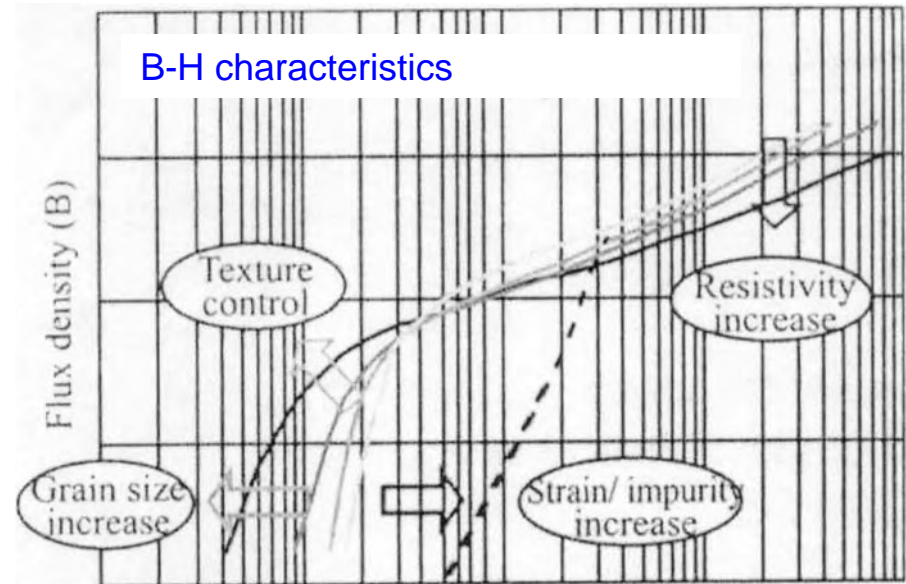
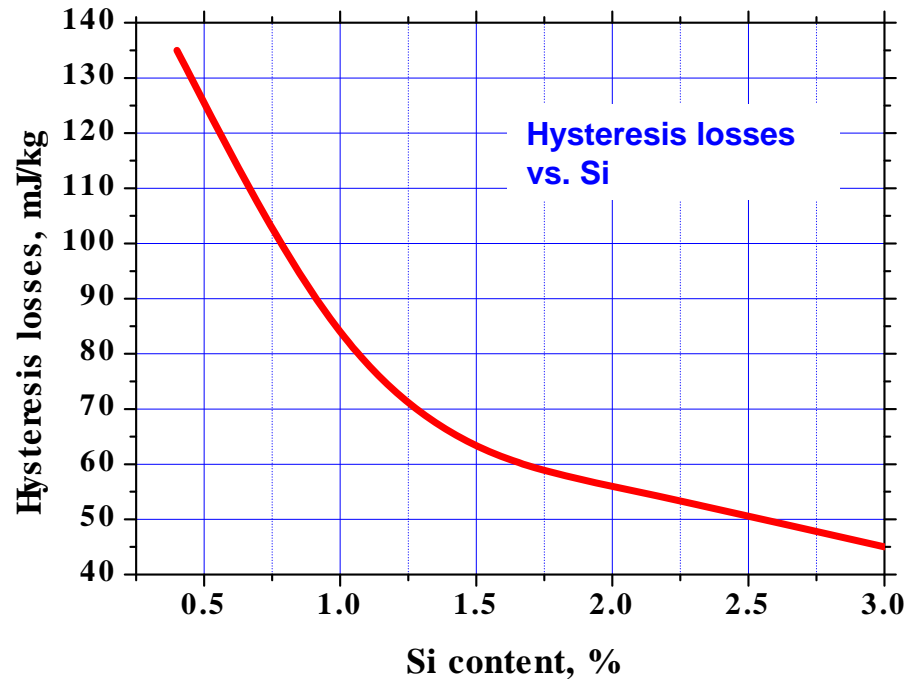
The search for this was made in both principle possible directions, i.e. analysing the intrinsic properties of the Si-donated Fe system as well as the available commercial steel. In the latter case also the impact of the technological and real application effects was discussed.

- **hysteresis losses:**
$$P_h = \frac{1}{2} k_h H_C B_{\max} \frac{dB}{dt}$$
 - **eddy current losses**
$$W_h = c_h B_{\max}^2 = \underbrace{k_h H_C}_{c_h} B_{\max}^2$$
 - **optimal B-H curve**
(high permeability at low B, high $M_s \sim 2.1 \text{ T}$)
- characteristic parameters:**
d thickness of steel sheet
 H_c coercive force
 μ_{\max} maximum permeability
 M_s magnetisation saturation
 W_{hyst} specific hysteresis losses
 ρ electric resistivity

Magnetic steel: Si content



Magnetic steel: Influence of Si



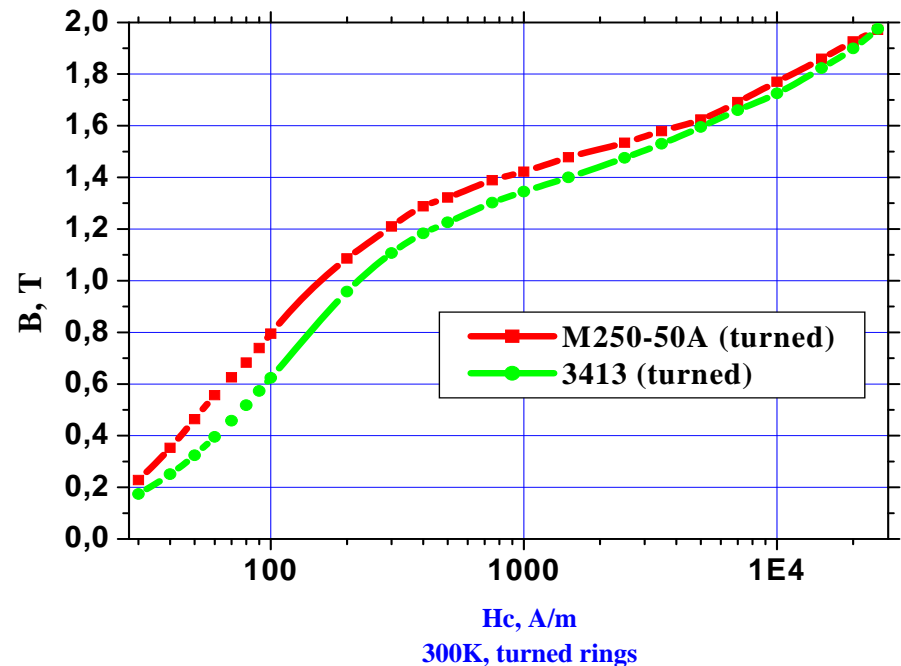
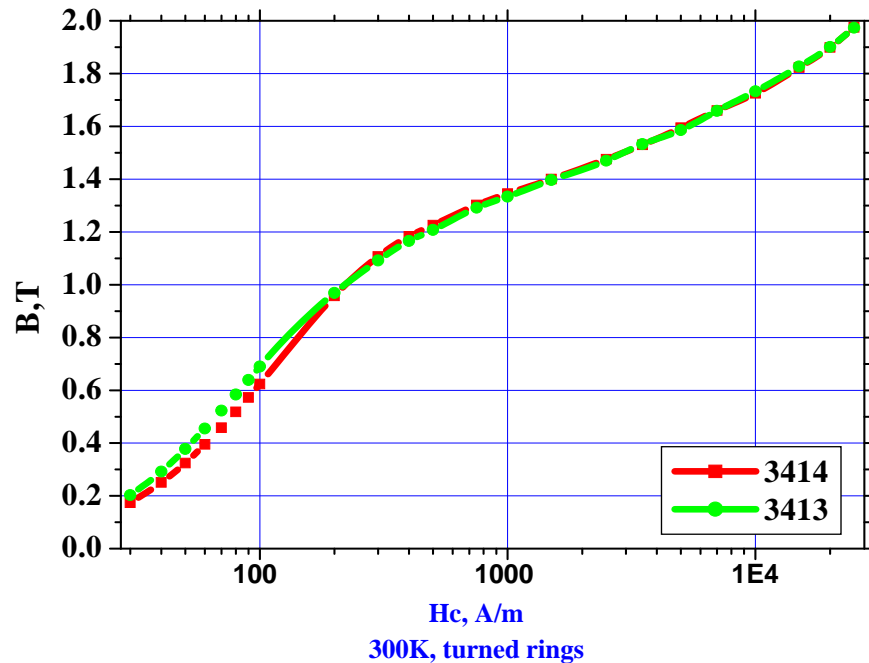
Parameter	Approximation function	unit
Saturation magnetization	$M_s = 2.16 - 0.048 \cdot \text{Si}$	T
Coercive force	$H_c = 120 - 30 \cdot \text{Si}$	A/m
Resistivity	$\rho = 0.1 + 0.12 \cdot \text{Si}$	$\mu\Omega\text{m}$
Density	$d = 7.865 - 0.065 \cdot \text{Si}$	kg/dm^3

◀ Dependence of the main parameters on Si content in %

1. Introduction
2. Main magnet components
3. Mechanical stability of the coil windings
4. Magnetic steel
 - Dependence on Si content
 - Steel Comparison
 - Selection
5. Magnetic field design
6. Losses and hydraulic limits
7. Vacuum chamber and temperature fields
8. Milestones towards a curved single layer dipole
9. Conclusion

Magnetic steel: Comparison of Si steels

Measurements: Hc and B-H curves



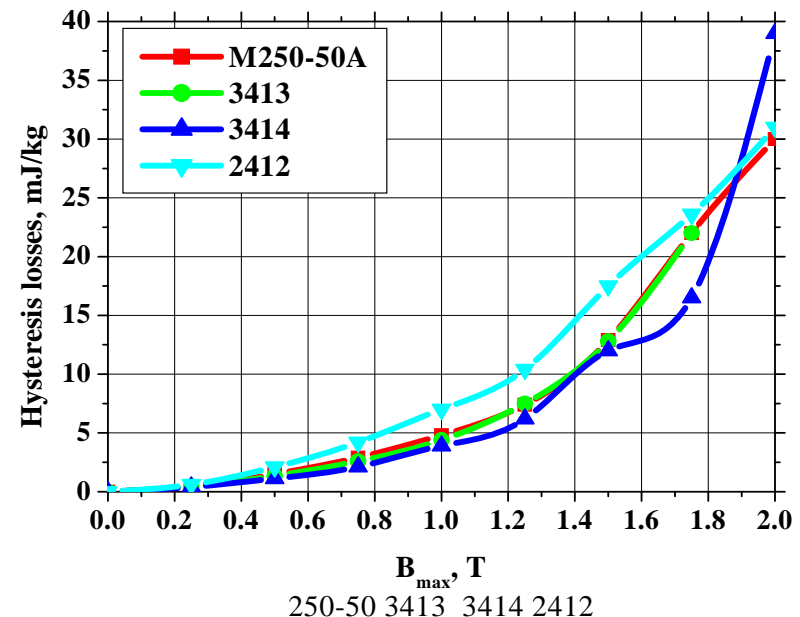
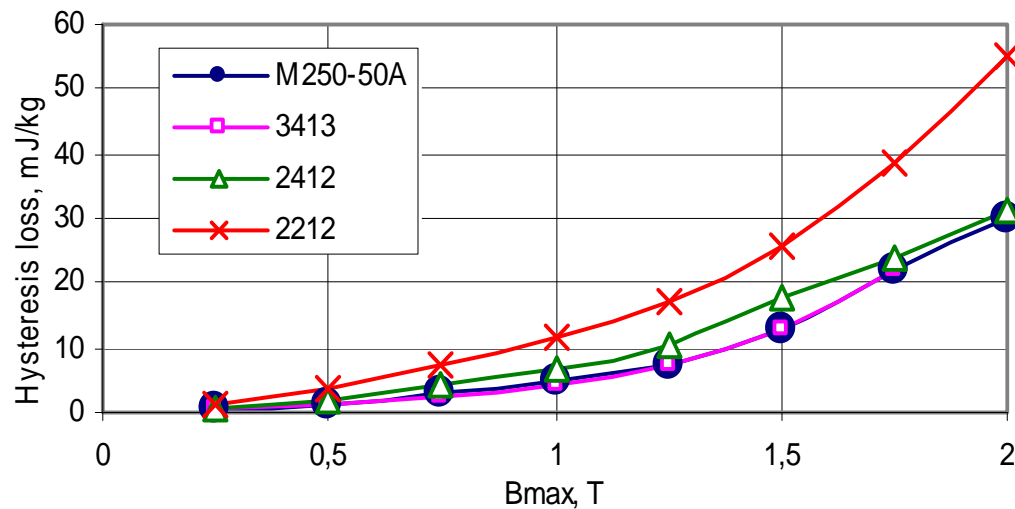
Hc	[A / m]	300 K	77 K	4.2 K
ET3413		21.3	20.8	21
ET3414		20.3	19.5	19.5
Stabocor M250-50A		31.53	30.5	30.9

Hc	[A / m]	Along rolling	Across rolling	Mixed
3413, $B_{\max} = 1.64$ T		16	48	28
3414, $B_{\max} = 1.64$ T		26	41	32
Stabocor M250-50A, $B_{\max} = 1.67$ T		30	50	39

Magnetic steel: Comparison of Si steels

Measured hysteresis loss in unipolar cycles 0 - B_{\max} at 4.2 K

Steel	ET3413	M250-50	M600-100	M700-100
M_s [T]	2.055	2.035	2.035	2.1
H_c [A/m]	20 – 30	30 – 33	30 – 33	35 - 40




1. Introduction
2. Main magnet components
3. Mechanical stability of the coil windings
4. Magnetic steel
 - Dependence on Si content
 - Steel Comparison
 - Selection
5. Magnetic field design
6. Losses and hydraulic limits
7. Vacuum chamber and temperature fields
8. Milestones towards a curved single layer dipole
9. Conclusion

Magnetic yoke: Selecting the steel

- There are large uncertainties in magnetic properties of steels and one should be very careful when optimising the 2D cross section:
 - measurement method (strip, rings, static (low frequencies) or 50 Hz);
 - anisotropy;
 - technology (production, stamping, turning);
 - operating temperature;
 - tension.
- An approved agreement about correct use is required by users of the B-H data and its recalculation for different cases.
- Accurate test measurements and detailed recalculations are required to obtain a high resolution magnetic field description.

Magnetic steel: Conclusion for steel selection

- Commercially available steels:
 - comparison: catalog and measurement data (GSI @ RT, IHEP @ RT, 4K)
- Hysteresis loss: isotropic and anisotropic comparable
 - thickness 0.5mm: M250-50 ↔ ET2414, ET3414
 - thickness 1 mm: M250-50 ↔ M600-100
- Steel development: costly, time consuming (not an option)
- Full size magnet: M700-100
- Natural choice : M250-50 or equivalent ET3414, ET2414
- Steel in series → requirements series production → e.g reliable material properties

- 
1. Introduction
 2. Main magnet components
 3. Mechanical stability of the coil windings
 4. Magnetic steel
 5. Magnetic field design
 6. Losses and hydraulic limits
 7. Vacuum chamber and temperature fields
 8. Milestones towards a curved single layer dipole
 9. Conclusion

Magnetic Field Description: Circular multipoles

Standard field description:

$$\mathbf{B}(\mathbf{z}) = B_y + iB_x = \sum_{m=0}^{\infty} \mathbf{C}_m \left(\frac{\mathbf{z}}{R_{ref}} \right)^m.$$

- convergent also outside R_{ref}
- satisfactory field description **only for analytical data**
- coefficients \rightarrow FT on data on R_{ref} (FEM, measurement) \rightarrow thus with artifacts

Magnetic Field Description: Elliptic multipoles

- allow to represent the field in the whole aperture of SIS 100 / NESR / CR
- allow to give a concise error propagation for rotating coil measurements in elliptic aperture
- allows to calculate circular multipoles within the ellipse

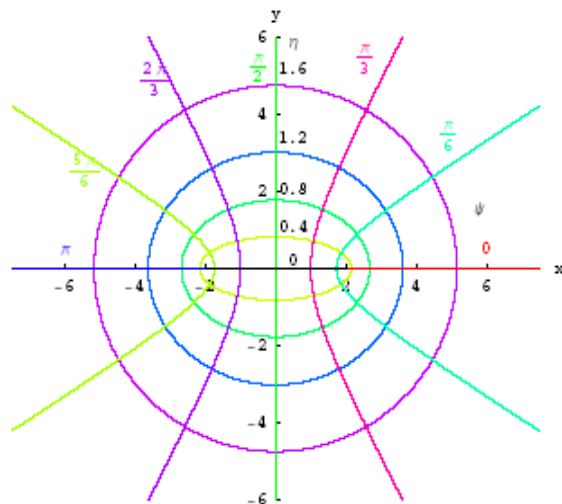
Field expansion:

$$w = \eta + i\psi$$

$$B(w) = \frac{e_0}{2} + \sum_{n=1}^{\infty} e_n \frac{\cosh[n(\eta + i\psi)]}{\cosh(n\eta_0)}$$

$\eta = \text{const.} \dots$ hyperbola

$\psi = \text{const.} \dots$ ellipse



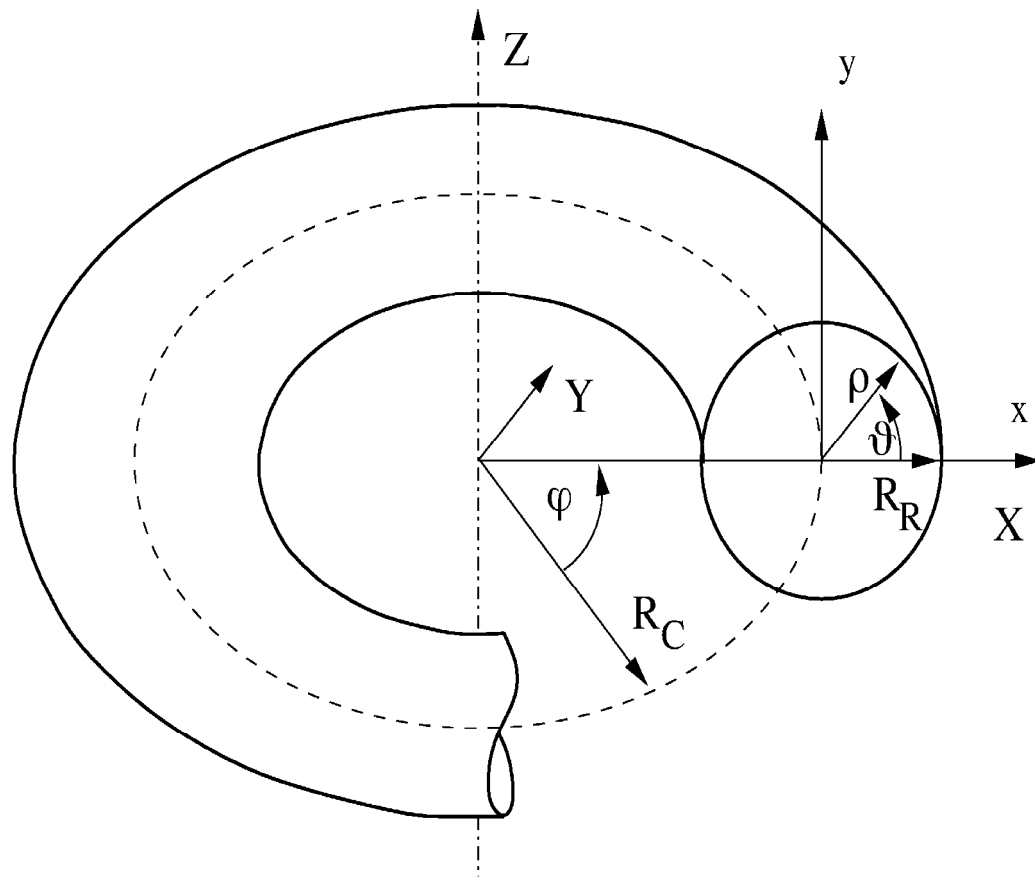
Plane elliptic coordinates η, ψ . Here the foci F, F' are at ± 2 .

Expansion coefficients:

$$e_n = \frac{1}{2\pi} \int_{-\pi}^{\pi} B(w = e \cosh(\eta_0 + i\psi)) \times \cos(n\psi) d\psi.$$

Linear Analytic Transformation to Circular Ones

Magnetic Field Description: Toroidal multipoles



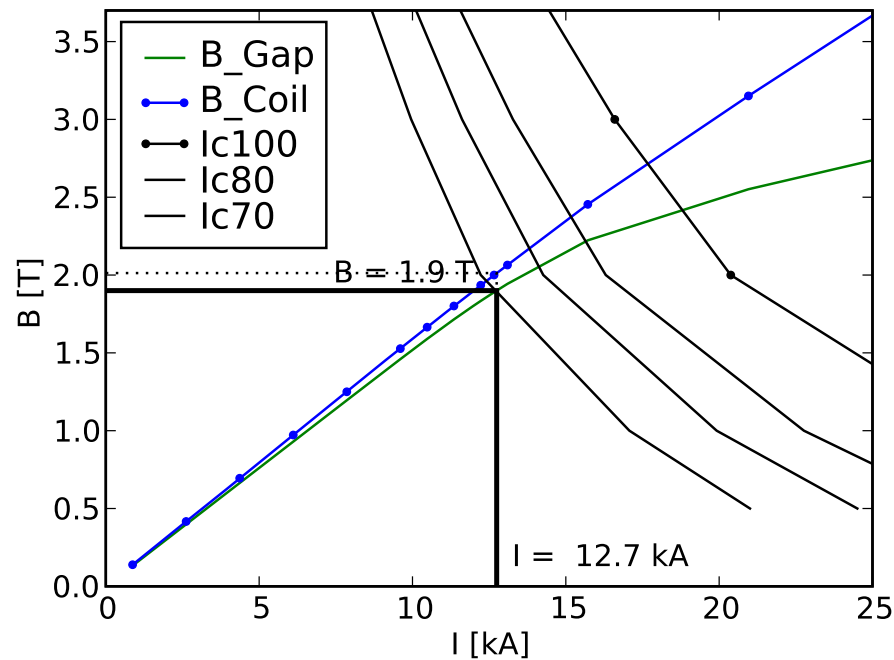
Local Toroidal Coordinates ρ, ϑ, ϕ

$$X + iY = R_c h e^{i\phi}$$

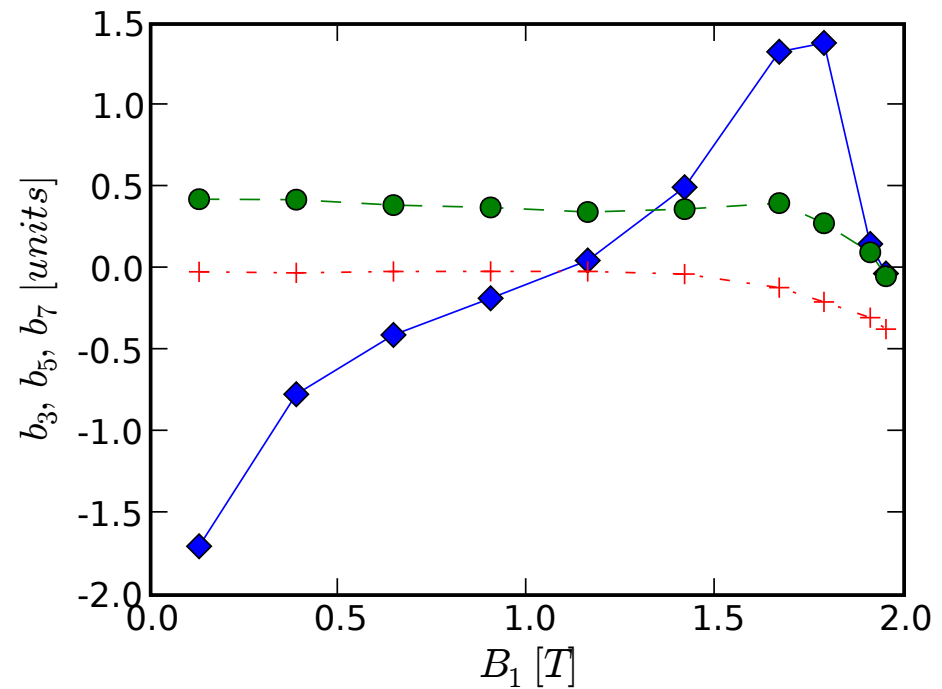
$$h = 1 + \varepsilon \rho \sinh \vartheta$$

$$\varepsilon = R_R / R_c \ll 1$$

Magnetic Field: 2D calculations for the CSLD



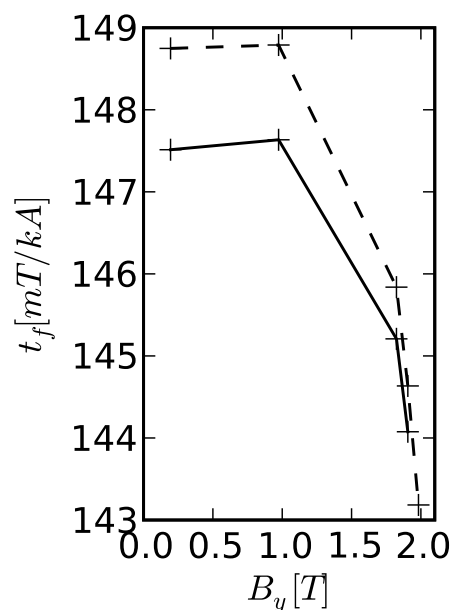
load line and margin



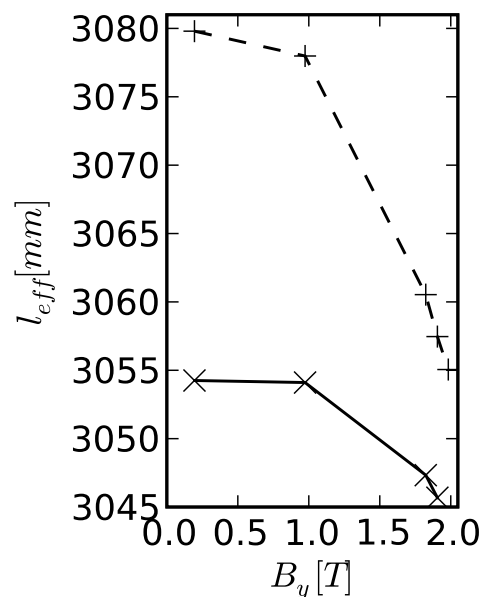
b_3 , b_5 , b_7

Magnetic Field: 3D Field quality

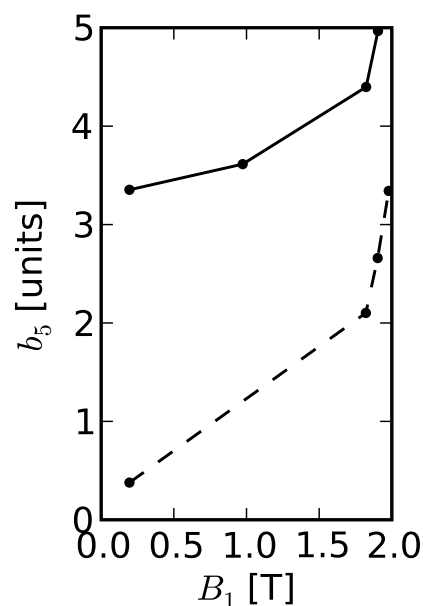
Calculated characteristics of the CSLD



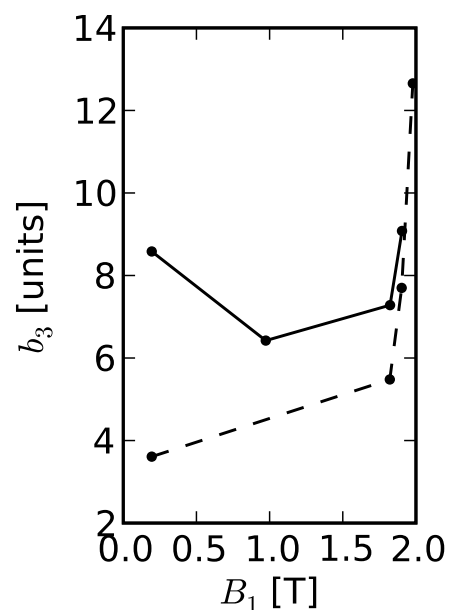
transfer function,
centre



transfer function,
length



b_3



b_5

- Rogowsky profil
- Rectangular ends

iron non linearity → 4 %

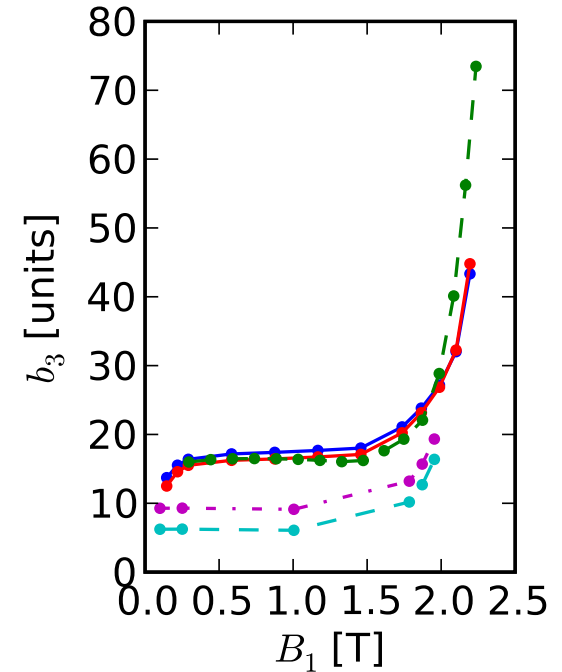
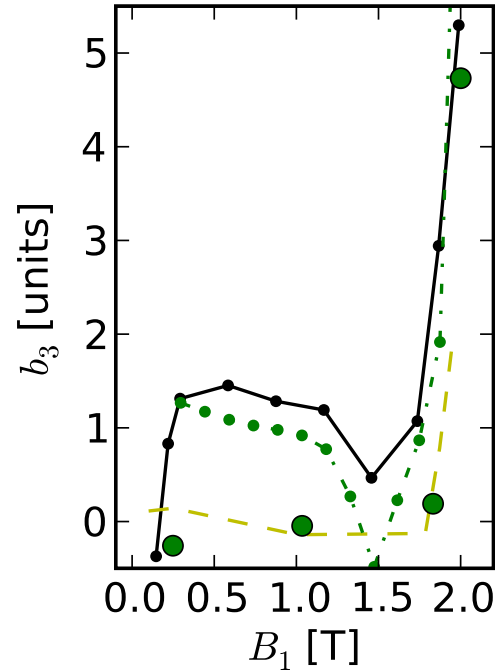
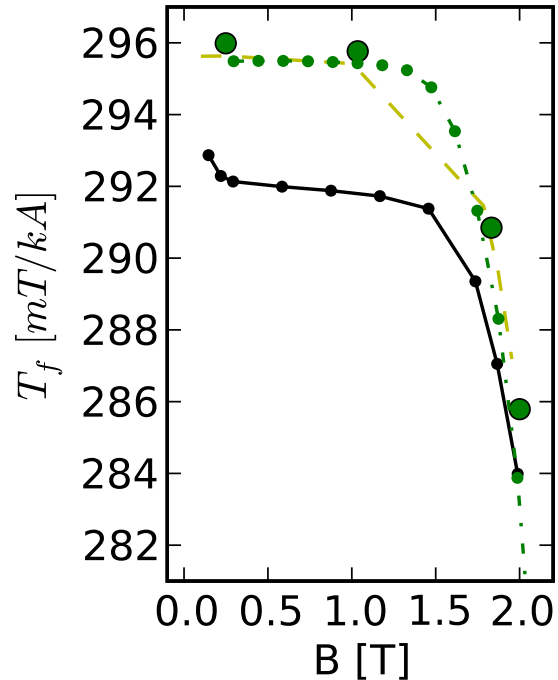
rectangular end → 1 %

Rogowsky end → 0.5 %

Calculation quality and measurement results

- Curved single layer dipole
 - not yet built
 - presented data → calculations
- First full size dipole
 - thoroughly measured → mole, mapper
 - multipoles calculated → distributed
(e.g. beam dynamics calculations)
- Comparison: measurements ↔ calculations

Magnetic Field: S2LD-calculation & measurements

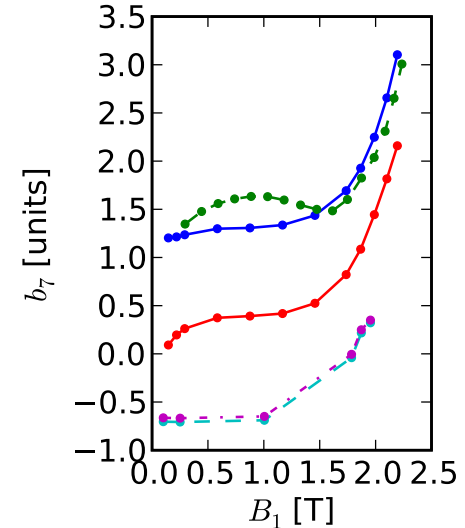
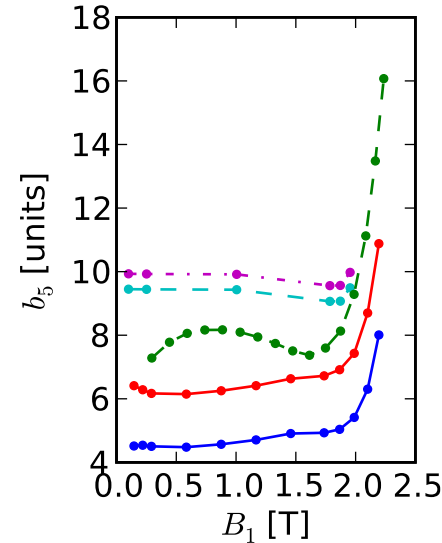
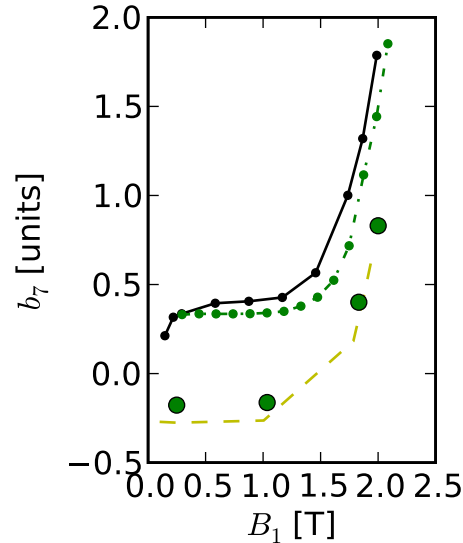
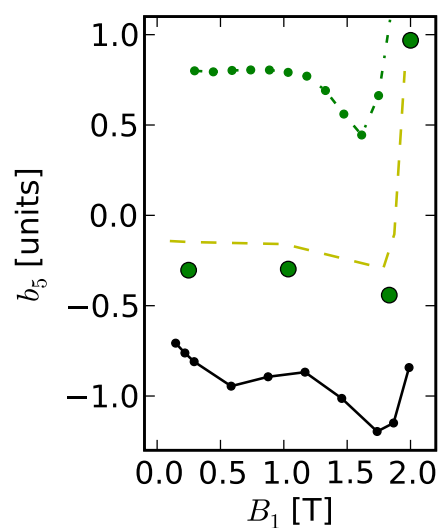


Centre: black: measurement
green: ANSYS (2 models)
yellow: TOSCA 3D

End CS: blue : measurement
cyan: TOSCA 3D
green: ANSYS

End NCS: red : measurement
magenta: TOSCA 3D
green: ANSYS

Magnetic Field: S2LD-calculation & measurements



Centre: black: measurement
green: ANSYS (2 models)
yellow: TOSCA 3D

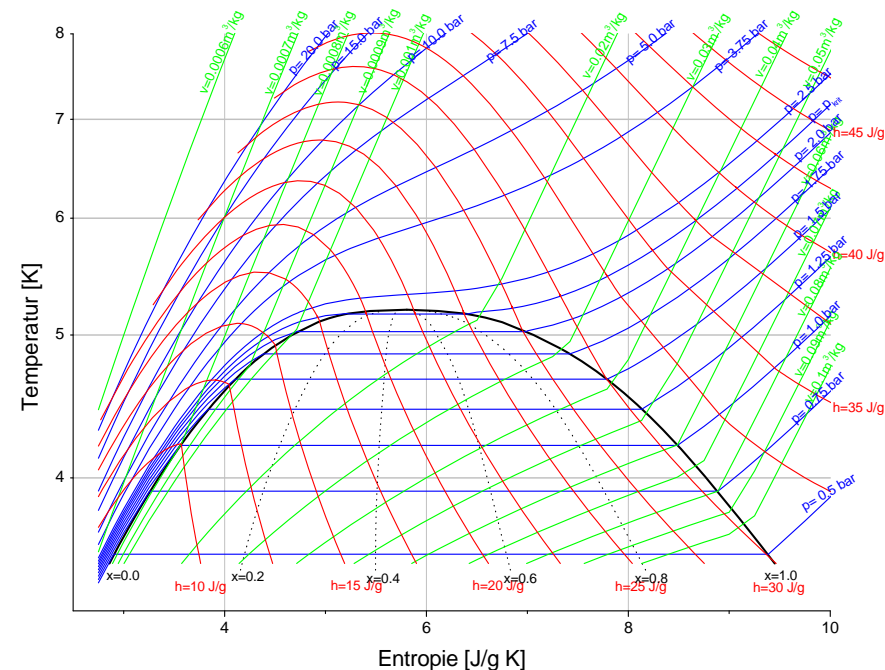
End CS: blue : measurement
cyan: TOSCA 3D
green: ANSYS

End NCS: red : measurement
magenta: TOSCA 3D
green: ANSYS

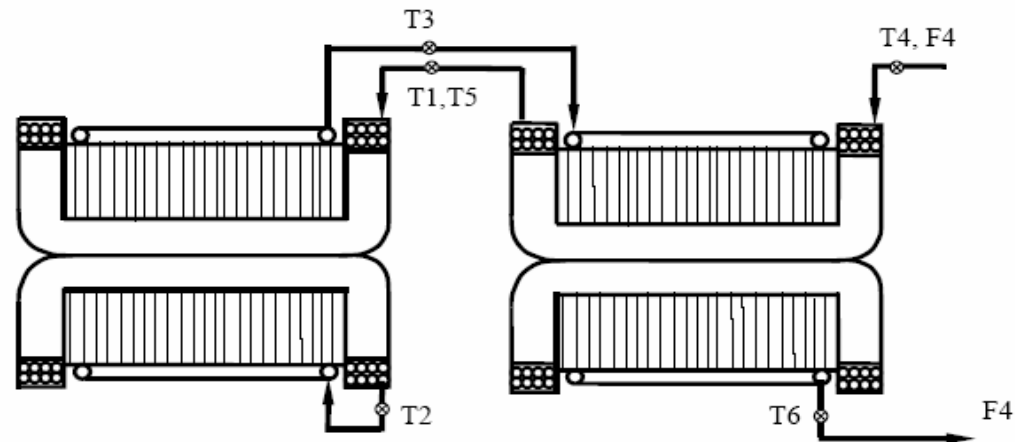
1. Introduction
2. Main magnet components
3. Mechanical stability of the coil windings
4. Magnetic steel
5. Magnetic field design
6. Losses and hydraulic limits
 - measurement on equivalent model
 - consequences for the coil design
 - BNG magnet: measured losses and parameterisation
7. Vacuum chamber and temperature fields
8. Milestones towards a curved single layer dipole
9. Conclusion

Losses & hydraulics: equivalent model

The hydraulic resistance of the coil limits the feasibility of the cycles!



T – S phase diagrams for He^4

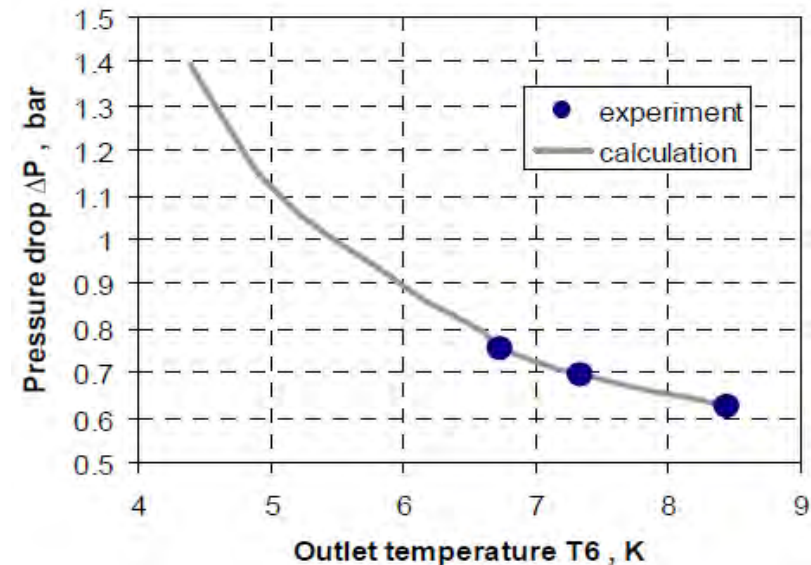
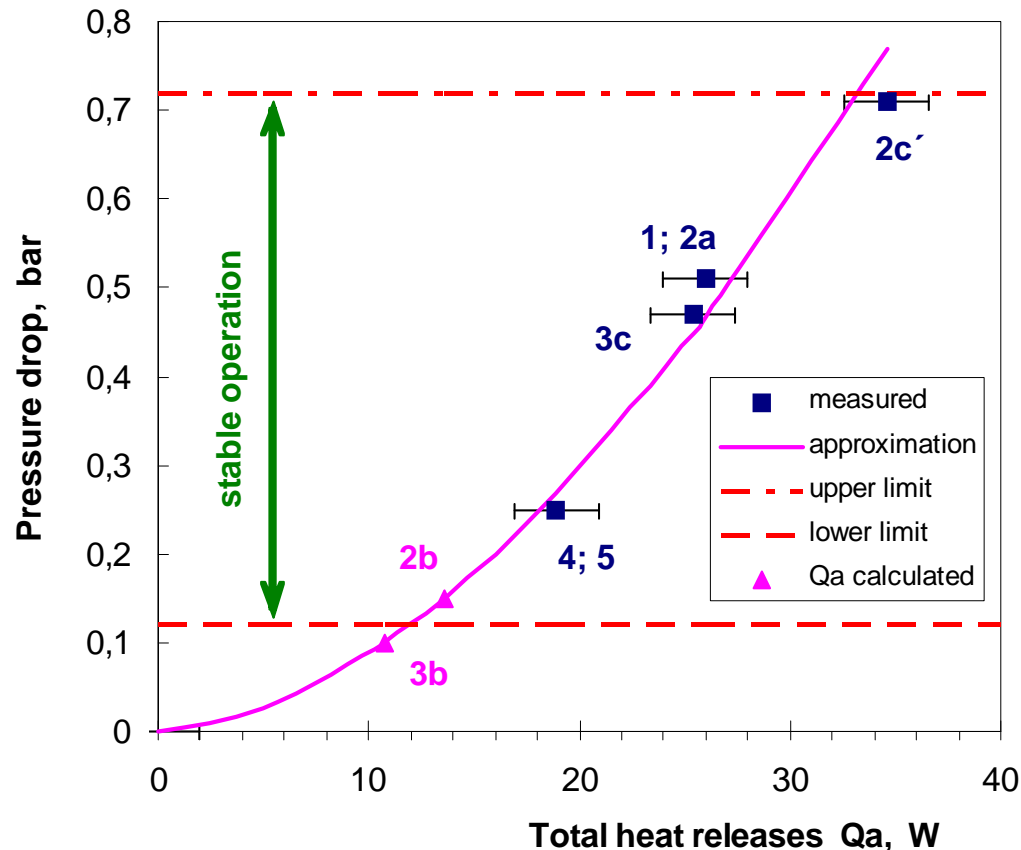


Cooling schema of the equivalent dipole model:

T1, T2, . . . T6 – temperature measurement points,
F4 - measured helium flow. The two-phase helium
flow enters the laminated yoke after cooling the
two short coils all connected in series.

Losses & hydraulics: feasible cycles

The hydraulic resistance of the coil limits the feasible cycles!



Confirmed by the Measurements on the Full Size Straight Dipole (BNG)

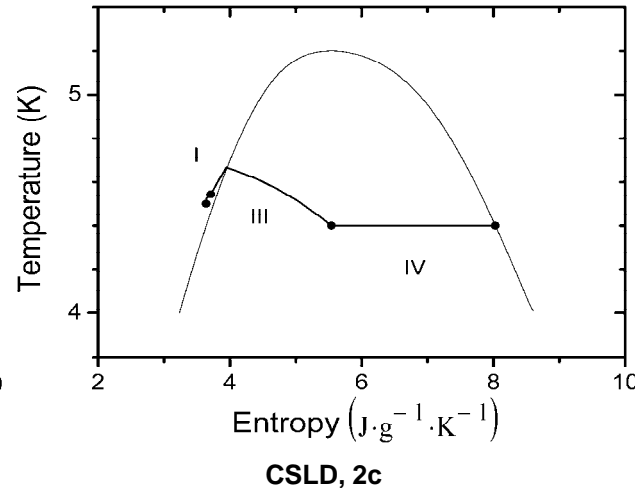
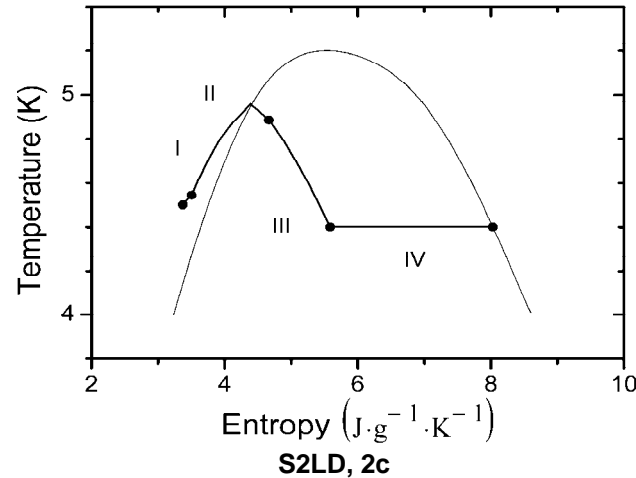
1. Introduction
2. Main magnet components
3. Mechanical stability of the coil windings
4. Magnetic steel
5. Magnetic field design
6. Losses and hydraulic limits
 - measurement on equivalent model
 - consequences for the coil design
 - BNG magnet: measured losses and parameterisation
7. Vacuum chamber and temperature fields
8. Milestones towards a curved single layer dipole
9. Conclusion

Losses & hydraulics: alternatives

<i>Parameter \ Version</i>	straight	curved	C2LD-a	CSLD
Maximum field, T	2.11	1.9	1.9	1.9
Magnetic length, Tm	2.756	3.062	3.062	3.062
Turns per coil	16	16	16	8
Usable aperture, mm ²	130 · 60	115 · 60	115 · 60	140 · 60
<i>Cables</i>				
Number of strands	31	31	38	23
Outer diameter, mm	7.36	7.36	7.5	8.25
Cooling tube inner diameter, mm	4	4	4.7	4.7
Length of the cable in the coil, m	110	110	110	57
Bus bars length, m	37	39	39	39
Operating current	7163	6500	6500	13000
Critical current @ 2.1 T, 4.7 K	11900	11900	11900	19840
<i>Wires</i>				
Strand diameter, mm	0.5	0.5	0.46	0.8
Filament diameter, µm	2.5 - 4	2.5 - 4	2.5 - 4	3.5 - 4
Filament twist pitch, mm	4 - 5	4 - 5	4 - 5	5 - 8
<i>loss and hydraulic</i>				
Static heat flow, W	7	7	7	7
Heat load to bus bars, W	0.5	0.5	0.5	0.5
	<i>cycle 2c</i>			
AC losses, W	36.3	35.4	35.4	35.7
Pressure drop, bar	1.10	1.15	0.604	0.389
T _{max} of He in the coil (for x ₆ ≈ 1), K	4.94	4.95	4.78	4.64
	<i>triangular cycle [dB/dt = 4 T/s, t_{cycle} = 2 · B_{max} / (dB/dt)]</i>			
AC losses, W	75.1	74.0	74.0	74.6
Pressure drop, bar	1.14	1.20	0.657	0.486
T _{max} of He in the coil, K	5.08	5.10	4.86	4.72
	at T ₀ =8K	at T ₀ =8K	at T ₀ =8K	at T ₀ =7K

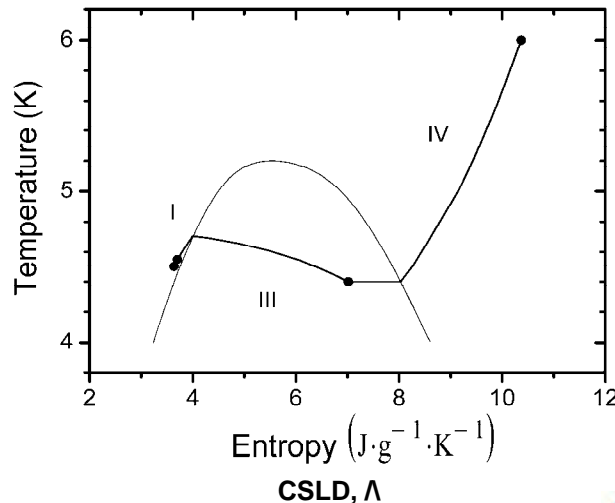
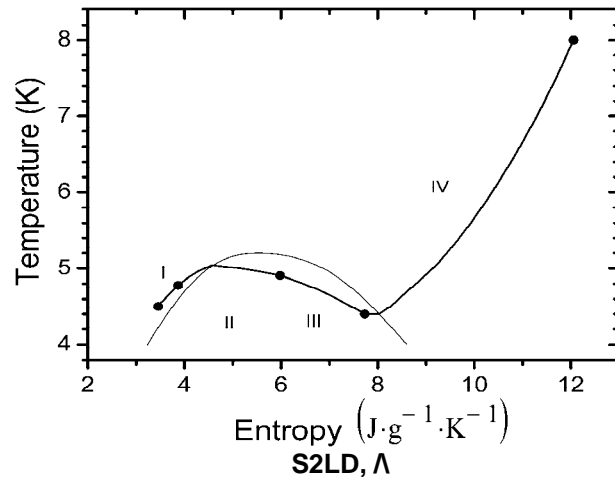
- The original Nuclotron cable had to be adapted for the main parameters of the SIS100 dipole.
- An optimisation of the sc wire characteristics is not sufficient.
- Even if the triangular cycle will not be requested, the design change was unavoidable due to the failure of cycle 2c !
- The optimal solution of the hydraulic boundary condition is the Curved Single Layer Dipole providing the continuously triangular cycle and a larger aperture for a stable and cryo cooled beam pipe with save margins.

Losses & hydraulics: phase diagram



The straight Two Layer Dipole (S2LD) and the Curved Single Layer Dipole (CSLD) at intensive ramping modes

new geometry of the cable \Rightarrow reducing hydraulic resistance \Rightarrow stable operating 2c and Λ cycle



T – S diagrams for the 2c and Λ operation

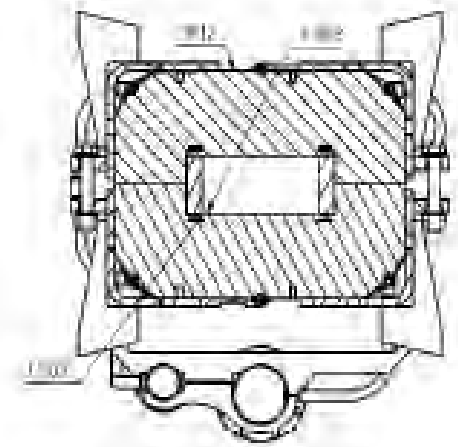
Helium flow trough the bus bars I, the coil II - III (inner - outer layer) and the iron yoke IV at cycles - 2c (left) and triangular (right)

1. Introduction
2. Main magnet components
3. Mechanical stability of the coil windings
4. Magnetic steel
5. Magnetic field design
6. Losses and hydraulic limits
 - measurement on equivalent model
 - consequences for the coil design
 - BNG magnet: measured losses and parameterisation
7. Vacuum chamber and temperature fields
8. Milestones towards a curved single layer dipole
9. Conclusion

Losses & hydraulics: AC losses for BNG dipole

dB/dt [T/s]	B_{max} [T]	t_d [s]	f [Hz]	P [W]	T_{out} [K]	dP [mbar]	TM08 [K]	TM09 [K]	TM11 [K]	TM12 [K]
1	2.1	0	0.23	30	6	640	6.5	7.6	6.4	6.1
1.5	1.4	0	0.51	30	5.75	658	6.34	7.5	6.2	5.9
1.5	1.6	0	0.44	33	6.49	667	6.9	7.8	6.8	6.5
1.5	1.9	0	0.31	35	7.12	674	7.4	8.1	7.3	7.0
1.5	2.1	0	0.33	37	7.8	691	7.9	8.4	7.9	7.5
2	1.9	0	0.49	43	9.6	735	9.2	9.4	9.2	8.9
2.5	2.1	0.8	0.37	41	8.9	740	8.8	9.1	8.9	8.5
3	1.9	0.8	0.45	43	9.2	780	9.0	9.3	9.1	8.7
3.5	1.9	0.8	0.49	43	9	775	8.9	9.1	9.0	8.5
4	1.9	1.6	0.37	40	8.4	733	8.3	8.7	8.4	8.0
4	2.1	1.5	0.39	43	8.08	793	8.1	6.9	8.3	7.7

- calorimetric method
- VI – method



AC loss: estimates and measurements for the FAIR cycles

cycle	B_{max} [T]	t_f [s]	f_c [Hz]	\bar{P}_t [W]	Q_t [J]	\bar{P}_v [W]	Q_v [J]	\bar{P}_m [W]	Q_m [J]	\bar{P}_{VI} [W]	\bar{P}_C [W]
1	1.2	0.1	0.71	26.8	40.4	10.7	15.9	14.6	22.7		
2a	1.2	0.1	0.71	26.8	40.4	10.7	15.9	14.6	22.7	16.4	18.
2b	0.5	0.1	1.00	4.8	7.8	3.5	4.4	3.6	5.9		
2c	2.0	0.1	0.55	49.1	92.3	14.9	28.1	34.7	65.5		
3a	1.2	1.3	0.38	14.4	40.4	5.8	15.9	7.8	22.7	9	12.
3b	0.5	1.0	0.53	2.5	7.8	1.8	4.4	1.9	5.9		
3c	2.0	1.7	0.29	26.3	92.3	8.0	28.1	18.6	65.5	23	24.
4	2.0	0.1	0.20	17.9	92.3	5.4	28.1	12.6	65.5	15	17.
5	2.0	0.1	0.20	17.9	92.3	5.4	28.1	12.6	65.5		
Λ	2.1	0	1.05	96.7	101.7	29.4	30.9	69.6	73		

Losses & hydraulics: parametrisation

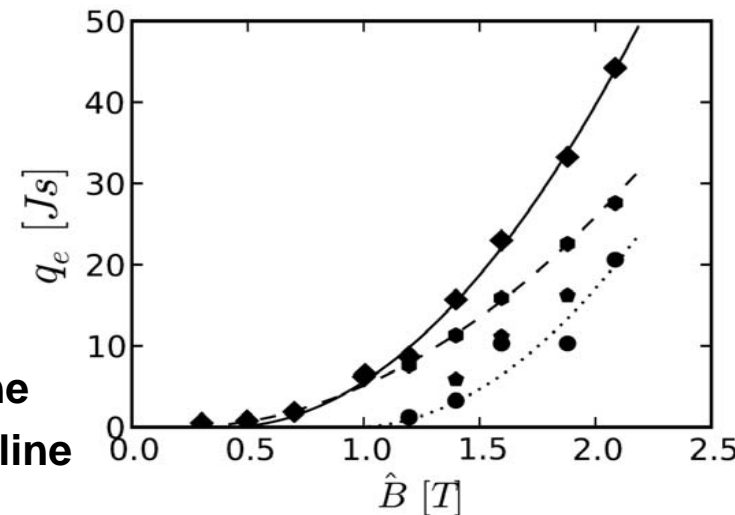
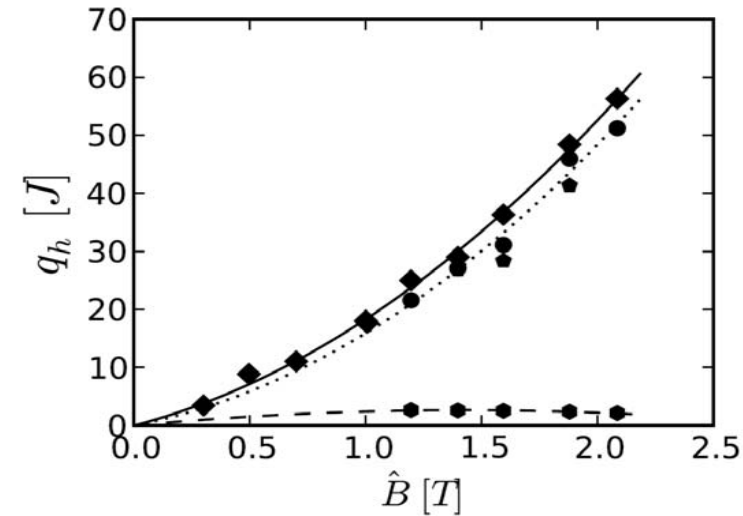
$$P_{\Lambda} = q_h(B_{max})f + q_e(B_{max})f^2 \quad f = 1/\tau_{\Lambda}$$

$$q_h = h_a B_{max} + h_b B_{max}^2 \quad q_e = \begin{cases} 0 & B_{max} < B_{th} \\ e_a (B_{max} - B_{th})^2 & B_{max} \geq B_{th} \end{cases}$$

Component	h_a	h_b	e_a	B_{th}
Magnet	7.6	8.3	15.5	0.95
Vacuum Chamber	3.7	-1.3	8.0	0.2
Total	10.3	8.3	15.5	0.4

results agree well with
calculations (ANSYS,
extrapolation from short
model magnet measurements)

magnet – dotted line
VC – dashed line
magnet + VC – solid line




Losses & hydraulic: potential reduction

Extrapolation to the curved single layer dipole

for Λ cycle

- Cable \rightarrow low loss wire $\approx 10 \text{ W} \downarrow$
- Yoke steel \rightarrow M700-100 (BNG) \rightarrow M600-100 $\approx 12 \text{ W} \downarrow$
- Magnet ends \rightarrow rectangular \rightarrow
eddy current reduction $\approx 7 \text{ W} \downarrow$
- Vacuum chamber cooling \rightarrow conduction cooling $\approx 6 \text{ W} \downarrow$
- Total $\approx 35 \text{ W} \downarrow$

- 
1. Introduction
 2. Main magnet components
 3. Mechanical stability of the coil windings
 4. Magnetic steel
 5. Magnetic field design
 6. Losses and hydraulic limits
 7. Vacuum chamber and temperature fields
 8. Milestones towards a curved single layer dipole
 9. Conclusion

Vacuum chamber: requirements

cryopump functionality for the operation with high intensity intermediate charge state heavy ions:

- ❶ cold surface → cryogenic adsorption pump 10^{-12} mbar for 20 years, infinitely refreshable
- ❷ ramped field → eddy currents in conducting materials → AC losses → field distortion
minimise by geometry and material selection
- ❸ mechanical stable → cryostat vacuum break (1 bara)
- ❹ beam image current
- ❺ shield beam (skin depth)

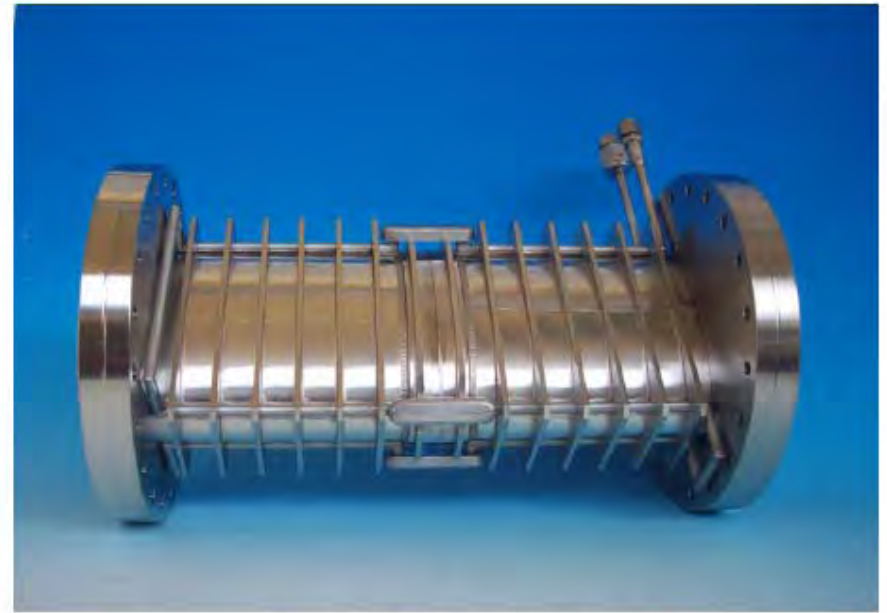
The vacuum chamber design was based on S. Wilfert, K. Keutel *SIS 100 Kryogene Vakuumkammern*
Otto-von-Guericke-Universität, 2004.

Vacuum chamber: current design

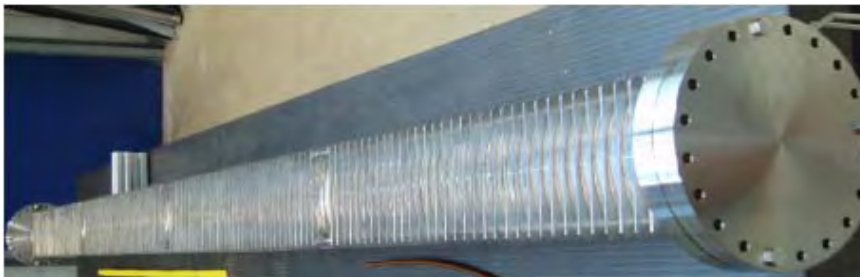
- cooling → separate tubes
- mechanis → ribs
- field distortion → stainless steel (Böhler Uddenholm)

but

- eddy current loops (ribs + cooling tubes)?
- final temperature?
- contact to magnet / coil?



short model and full size test chamber of the BNG dipole with mechanical stabilizing ribs and additional cooling tubes



Vacuum chamber: measured temperatures

The temperature of the vacuum chamber for the different FAIR cycles at He flow 0.17 g/s

	B_{min} [T]	B_{max} [T]	dB/dt [T/s]	t_f [s]	t_p [s]	t_c [s]	T_{in} [K]	T_{out} [K]
2a	0.24	1.2	4.0	0.1	0.70	1.408	5.12	15.46
3a	0.24	1.2	4.0	1.3	0.70	2.608	5.09	10.03
3c	0.24	2.0	4.0	1.7	0.68	3.408	5.14	12.66
4	0.24	2.0	4.0	0.1	3.88	5.008	5.09	9.84
2b	0.24	2.0	4.0	0.1	1.	1.4	magnet can not be operated in these cycles	
2c	0.24	2.0	4.0	0.1	0.7	1.82		
\wedge	0	2.0	4.0	0	0	1		

The existing design for the vacuum chamber was tested at the first full size dipol:

- fulfills the requirements for cryo cooling the inner surface of the beam pipe below 15 K and is mechanically stable,

but:

- significant losses and additional cooling circuit
- magnetic field distortions



Alternatives ?

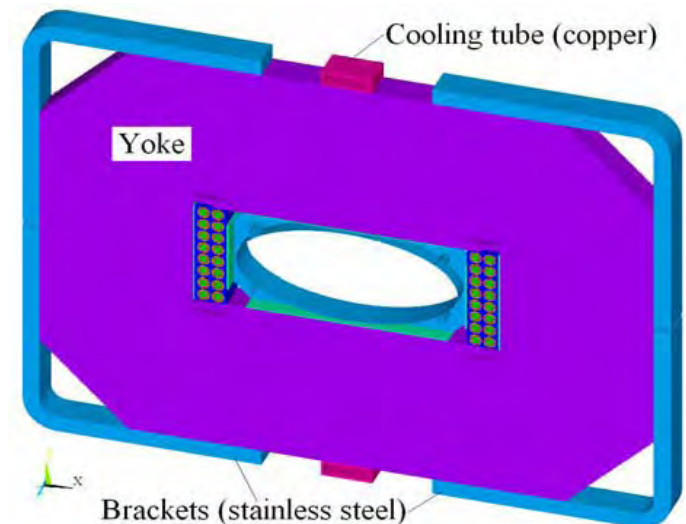
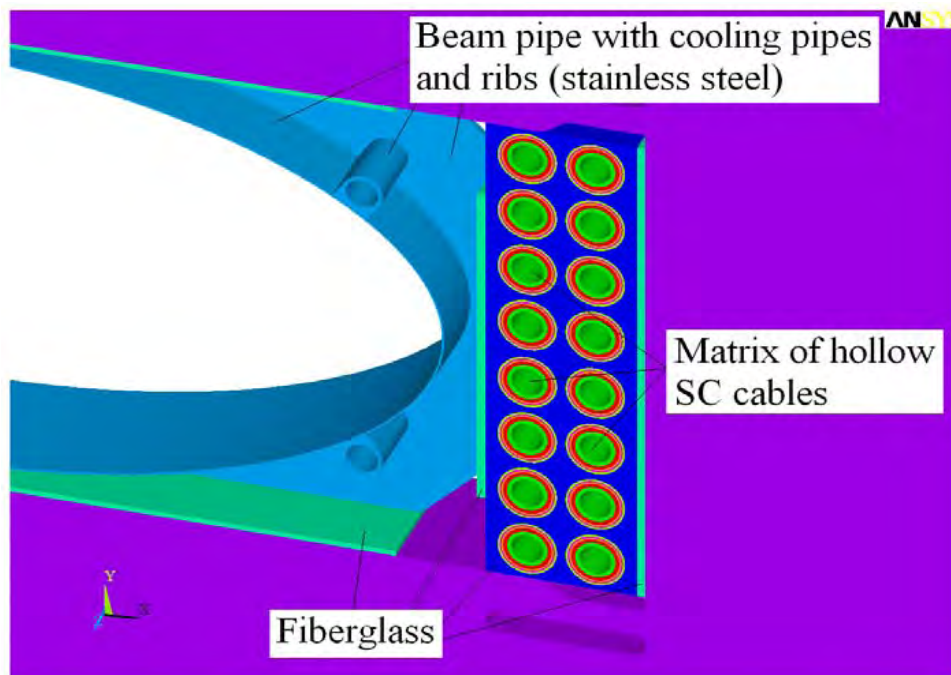
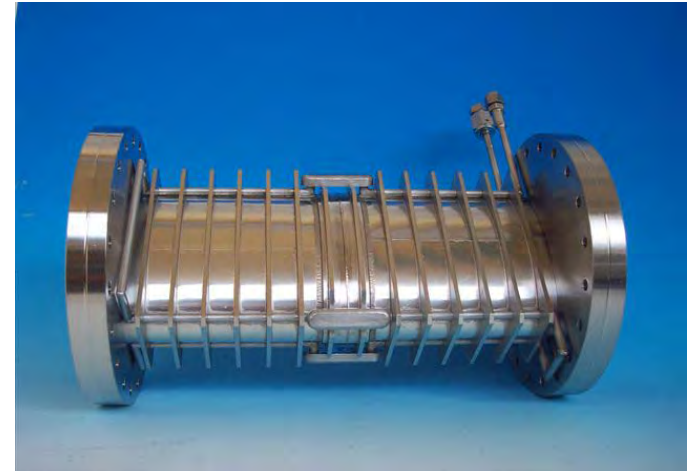
Vacuum chamber: temperature fields

Calculation Procedure

- vacuum chamber in defined contact with yoke and coil
- transient analysis steady state after 60 cycles
- used steady state mode for thermal calculations
- Different options studied
 - a) design as built by BNG
 - b) without coolant in the tubes
 - c) without ribs
- calculating the magnetic field within the vacuum chamber

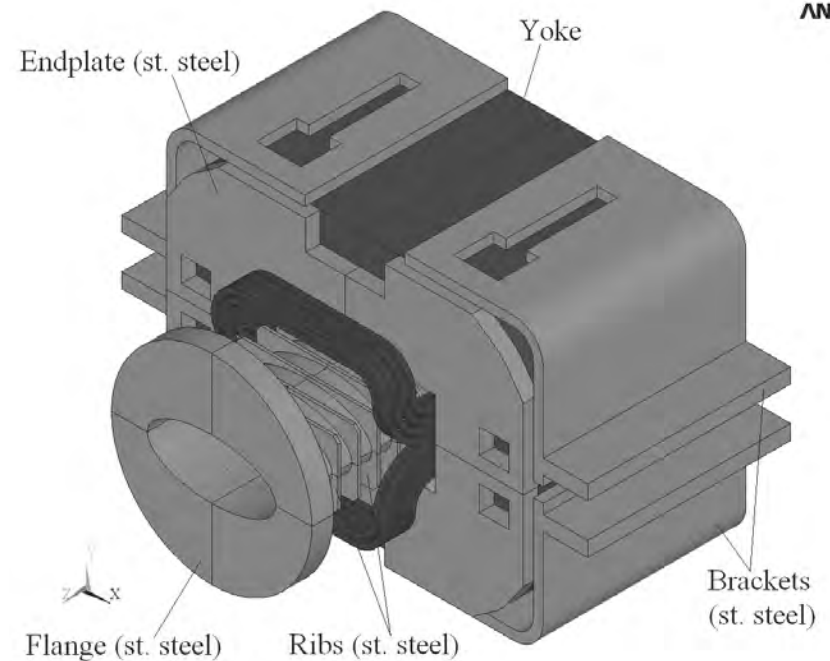
Vacuum chamber: temperature fields

- central part -- periodic "quasi 2D" model
- end part – 3D "short end model "
- transient analysis: steady state after 60 cycles
- Additional 25 W heat load (= 1/3 of the magnet)

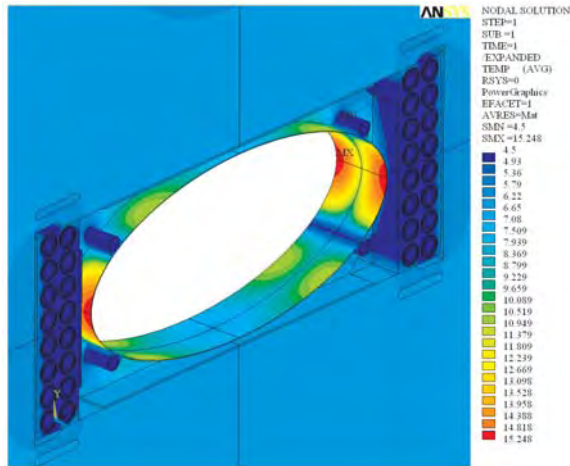


Vacuum chamber: Calculated average power

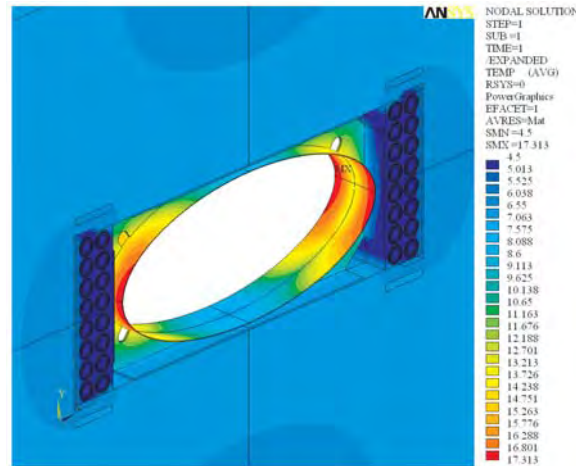
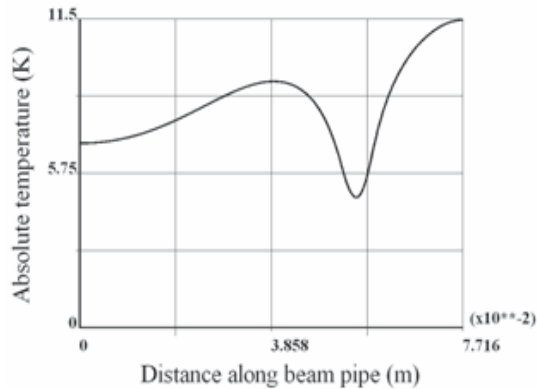
cycle	2a		2b		2c		\	
	H	E	H	E	H	E	H	E
<i>magnet central part</i>								
yoke	0.6	0.1	3.6		11.8	0.3	23.7	0.6
<i>magnet end part</i>								
brackets			0.4		0.7			1.2
endplates	1.1		3.3		3.8			8.0
yoke	0.4	0.8	1.5	2.2	3.0	4.0		5.3
<i>beam pipe central part</i>								
pipe	1.7		4.7		6.7			13.9
tubes	0.7		1.9		2.7			5.6
ribs	0.1		0.2		0.3			0.6
<i>beam pipe end part</i>								
pipe	0.3		0.7		0.9			1.9
<i>Total</i>								
magnet								
centre	0.7		3.9		12.2			24.5
end	1.8		6.0		9.7			18.5
coil	6		1		8			16
total	8.5		10.8		29.5			57.0
vacuum chamber								
	2.8		7.6		10.6			22.2
total load								
	11.2		18.4		40.5			79.1



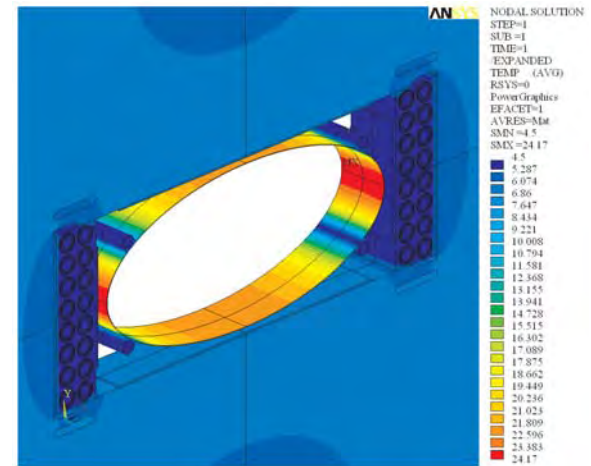
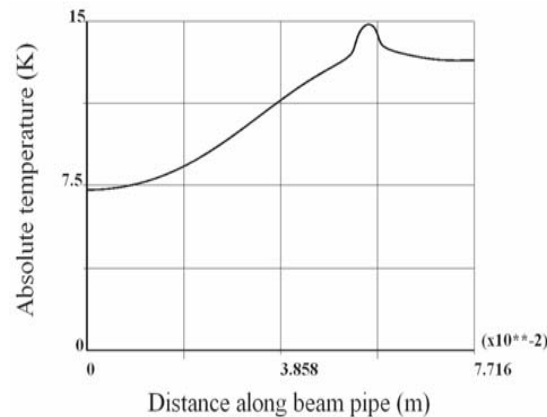
Vacuum chamber: Calculated temperatures



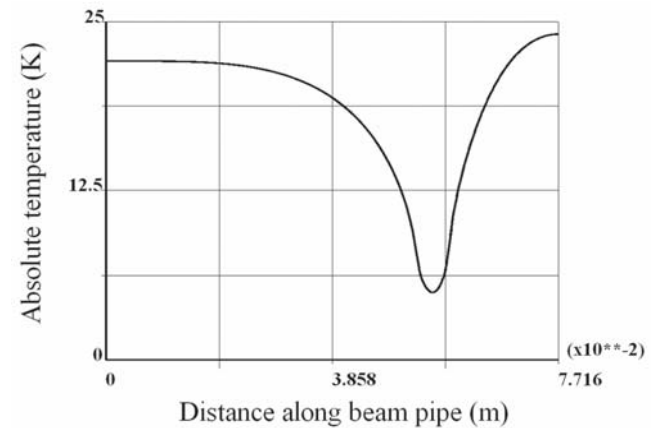
as a build



without coolant in the tube

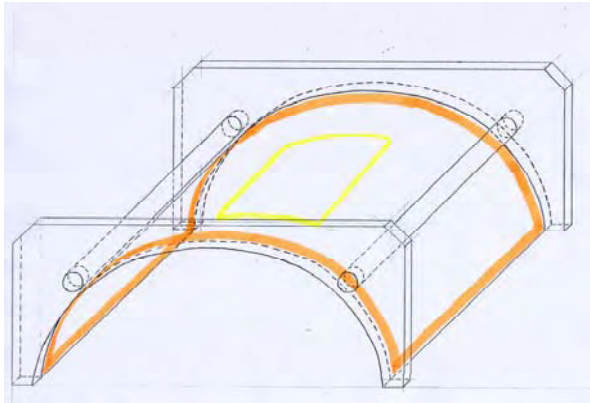


without rib

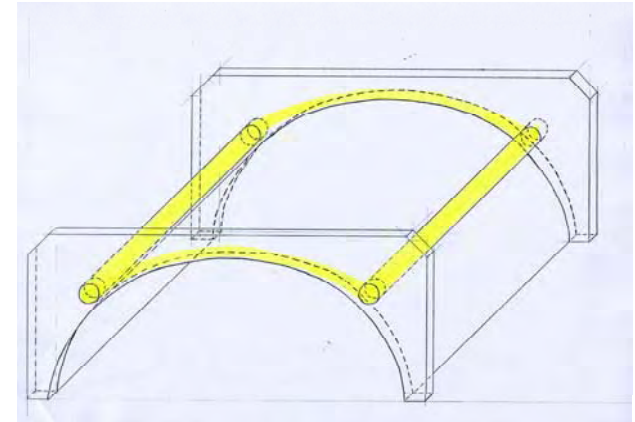


Vacuum chamber: Analytical model

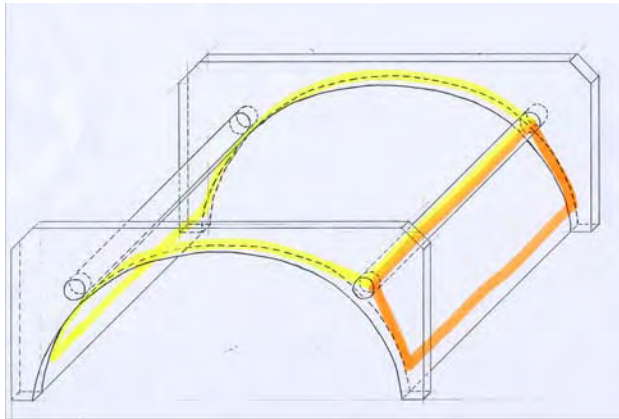
- Resistance of different components of VC and losses in the 4 cooling pipes



Loop1: vacuum chamber



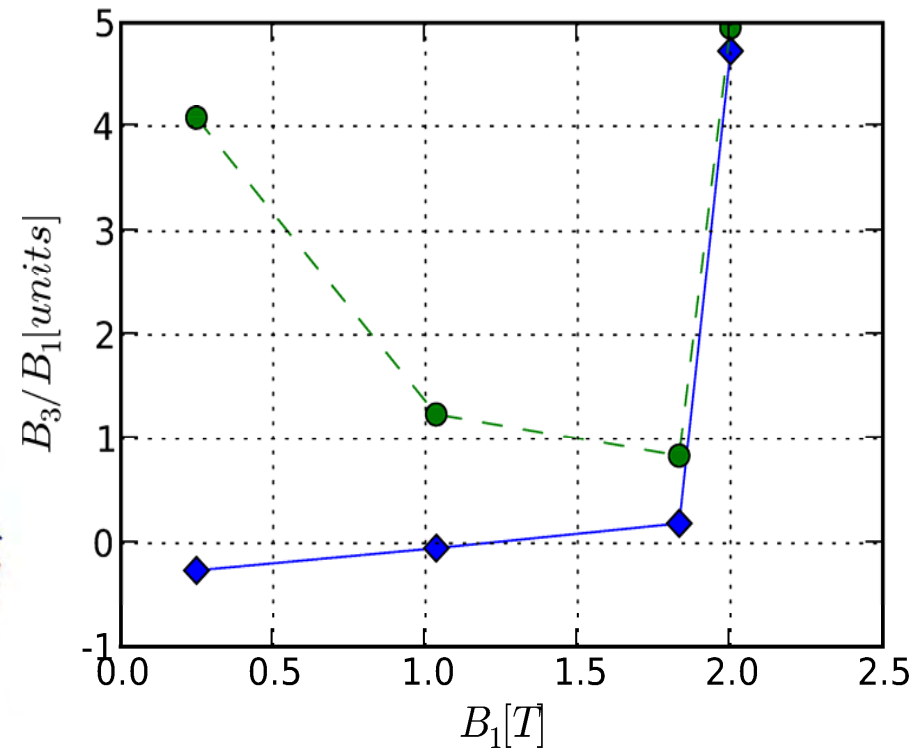
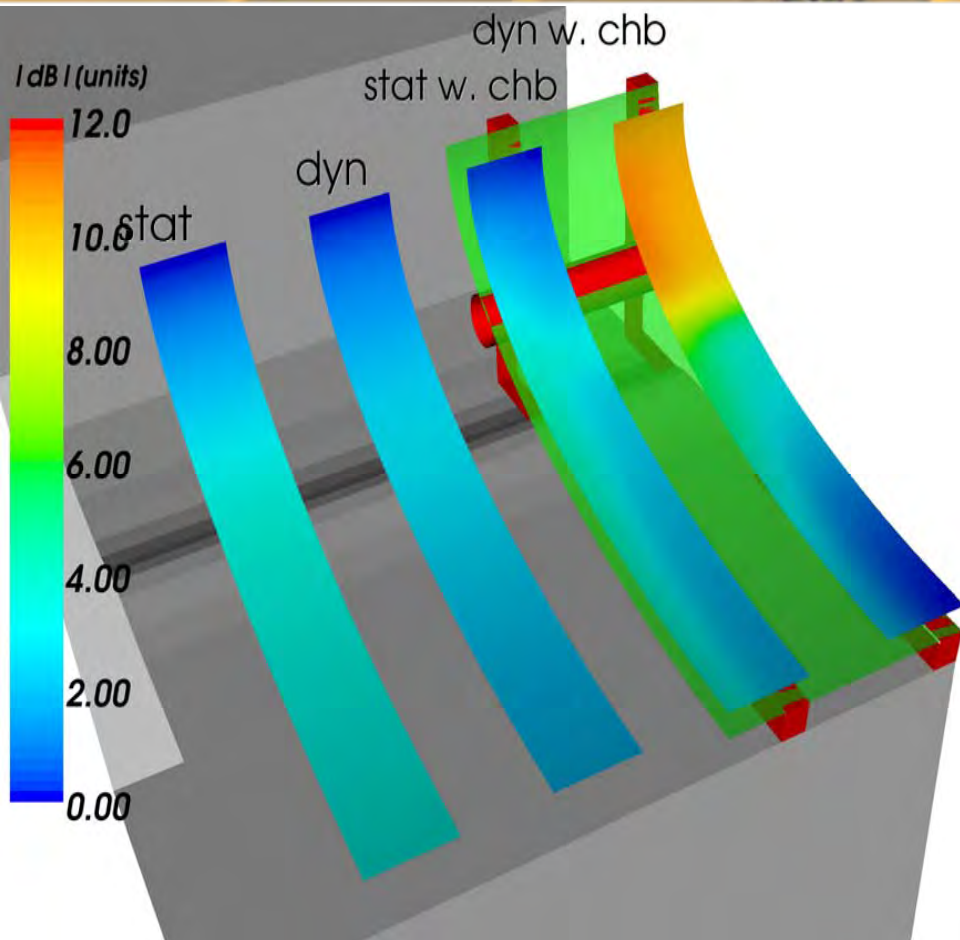
Loop2: pipe – rib - pipe



Loop3: chamber – rib - pipe

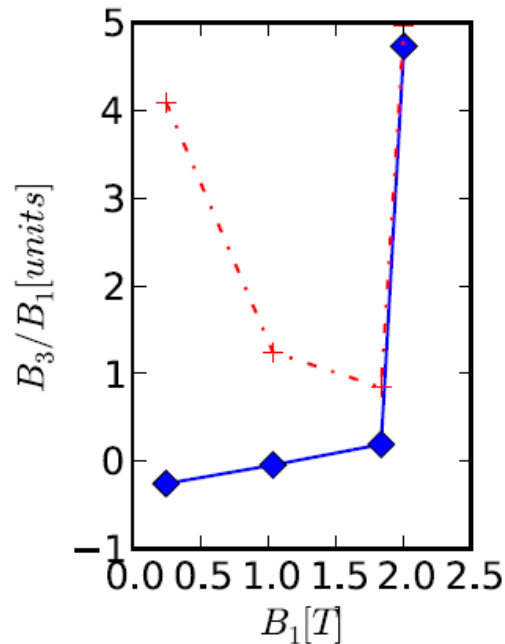
Part	decay constant τ μs	current A	resistance $\text{m}\Omega / \text{m}$	loss _{pipes} mW / m
chamber	22		5	
tubes	5		27	
Loop 1		0.1	30	2
Loop 2		2.7	variable	0.8
Loop 3		1.7	265	0.3

Vacuum chamber: Field deterioration

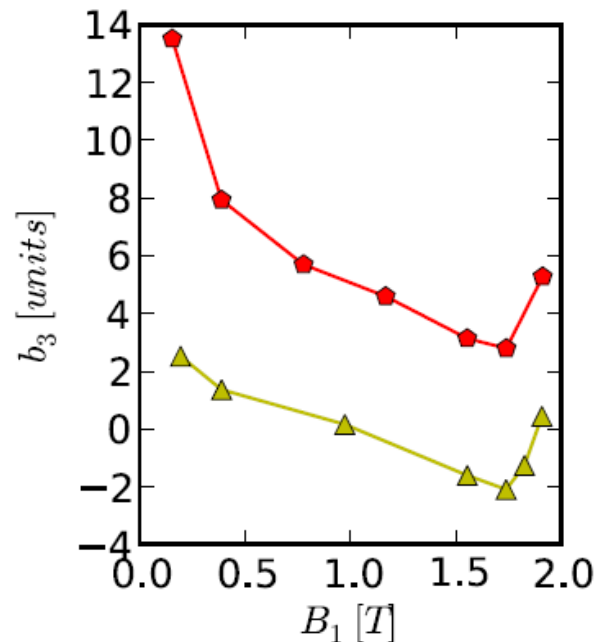


Vacuum chamber: ribs & cooling pipes
eddy currents large field deviation at
injection

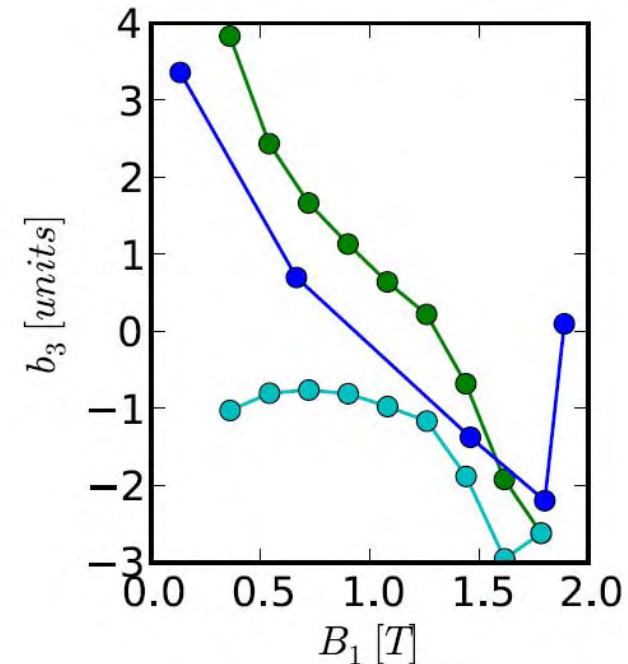
Sextupole



ANSYS, S2LD



OPERA 3D, CSLD



OPERA 2D, CSLD

S2LD with ANSYS

static – blue line
transient rump up – red line

OPERA 3D:

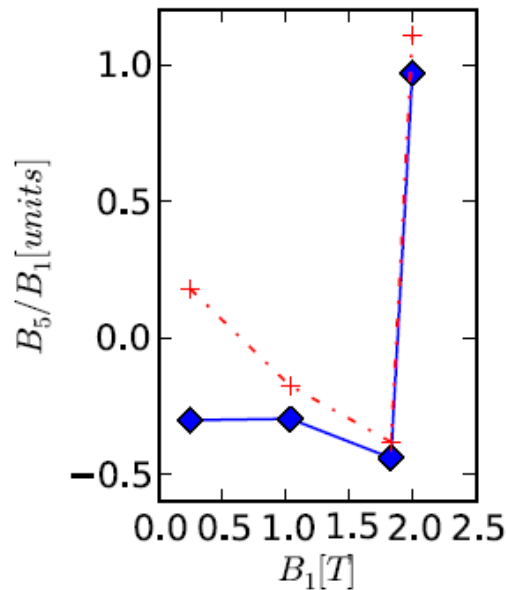
static – yellow line
transient rump up – red line

OPERA 2D:

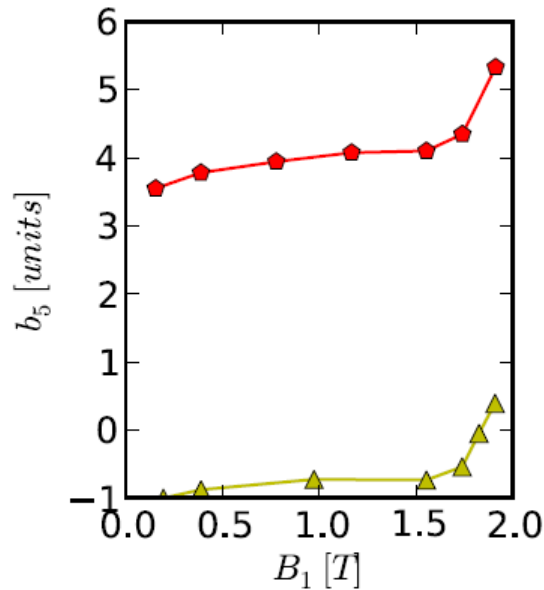
static – blue line
transient rump up – green line
transient rump down – cyan line

Vacuum Chamber: Field deterioration II/II

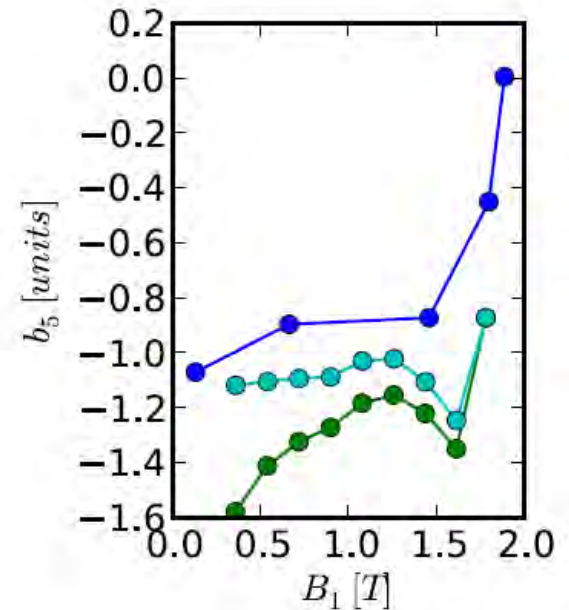
Dekapole



ANSYS, S2LD



OPERA 3D, CSLD



OPERA 2D, CSLD

S2LD with ANSYS

static – blue line
transient rump up – red line

OPERA 3D:

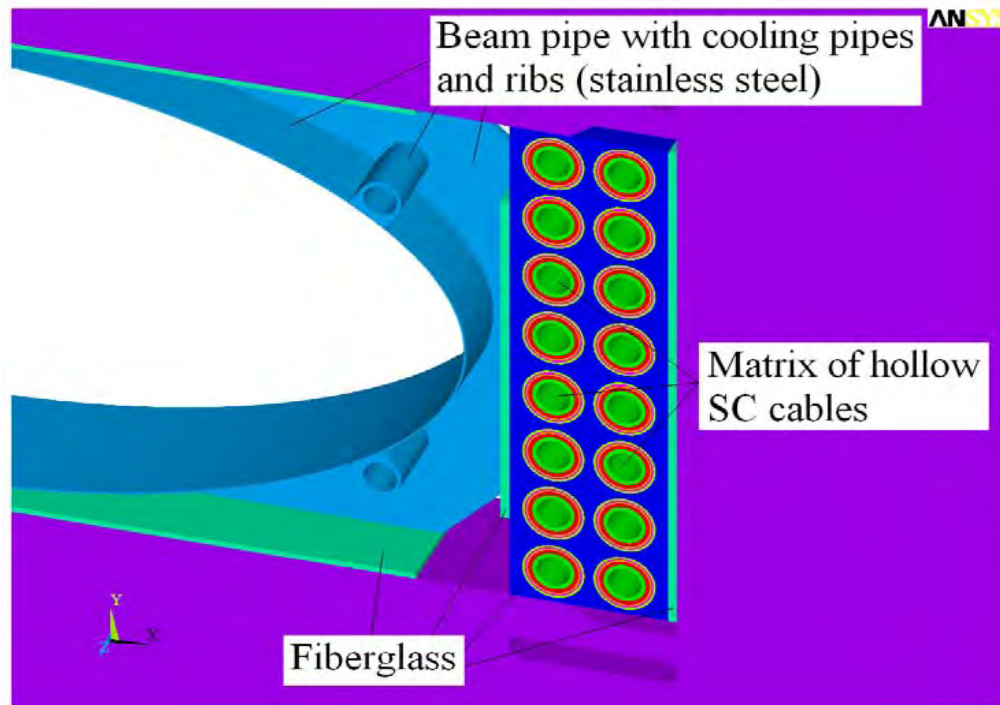
static – yellow line
transient rump up – red line

OPERA 2D:

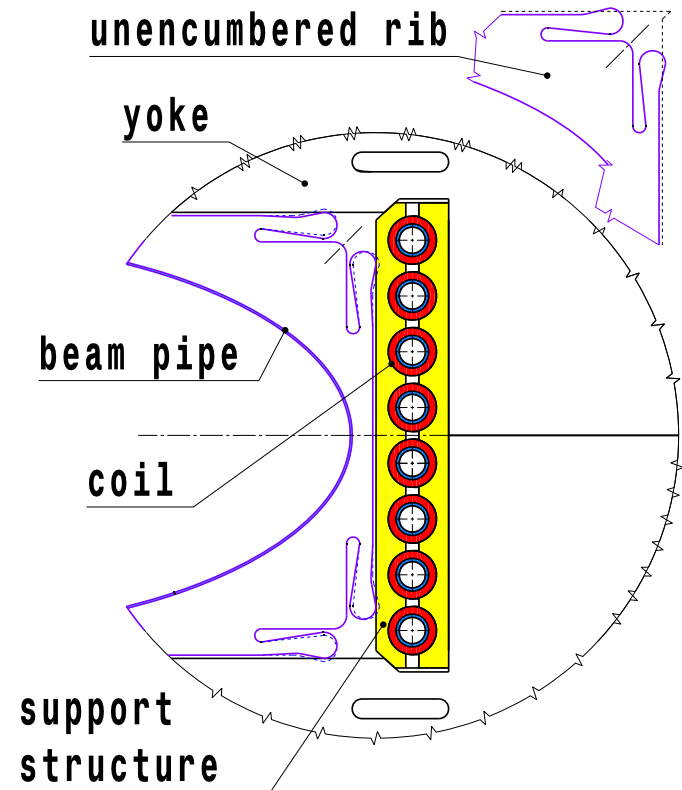
static – blue line
transient rump up – green line
transient rump down – cyan line

Vacuum Chamber: Cooling options

additional cooling ▼



Conduction cooling ▼

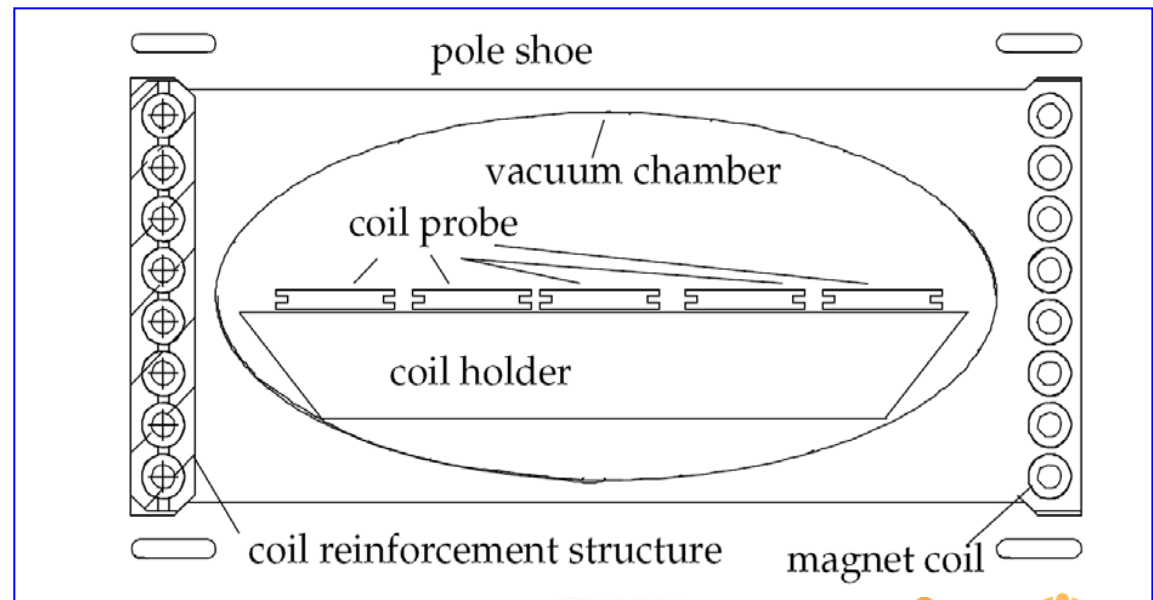



Stand: 09. Sept 2009

Elastic rib for
Dipole SIS100

Vacuum Chamber: Magnetic field measurement

1. Field → magnet measured without vacuum chamber
2. FEM model → adjust B-H curve → match field quality
3. Vacuum chamber → measured within nc magnet → material properties
4. VC installed in magnet → measured with “woodlouse”



- 
1. Introduction
 2. Main magnet components
 3. Mechanical stability of the coil windings
 4. Magnetic steel
 5. Magnetic field design
 6. Losses and hydraulic limits
 7. Vacuum chamber and temperature fields
 8. Milestones towards a curved single layer dipole
 9. Conclusion

2002	March: Decision to start high current Nuclotron cable larger aperture, hydraulic limits, AC losses
2003	Cooling power calculation; comparison to other cables Strands tested, design for 4 T magnet
2004	Dipole magnet with single layer coil → design and tested Nuclotron cable → strands direct contact to helium
2005	Nuclotron cable $\cos \theta$ magnet design → 4 T Review of SIS100 cooling concept
2006	Increase of magnet aperture for beam dynamics, triangular cycle hydraulic limits → necessitated single layer coil : presented at internal review Equivalent model test @ JINR / Dubna → confirming calculations Decision for 2 layer magnets (straight and curved)
2007	10 Hz Quadrupole, sc wire development for high current cable flexible cabling machine at BNG
2008	Status and limits of current SIS100 magnets presented at WAMSDO, ASC08
2009	Test of BNG magnet confirms predictions: no 2c High current cable: fabrication of wires

Conclusion

- The first SIS100 prototype dipole was intensively tested.
- The magnet training, the intensive long-term ramping stability, the measured current, the magnetic field characteristics as well as the AC-loss and cooling parameters have proven the preliminary design estimations and show that the applied production technologies are working well and ready for series production.
- These tests will be completed on a second straight dipole, a curved dipole utilising a two layer coil and on a prototype quadrupole with 6 coil per pole.
- The results obtained on the first prototype dipole confirm that our methodical design work is correct and the optimised curved single layer dipole is expected to fulfil all operation requirements for the SIS100 accelerator.
- This curved single layer dipole, while not yet built, is based on a sound R&D conducted since 2002.
- The next step toward final series production of the main magnets will be constructing and testing a curved dipole with a single layer coil made of high current superconducting cable.